Scuola Internazionale Superiore di Studi Avanzati
Trieste

Dynamic coupling between whisking, barrel cortex, and hippocampus during texture discrimination: A role for slow rhythms

Candidate:
Natalia Grion

Supervisor:
Prof. Mathew E. Diamond

Thesis submitted for the degree of Doctor of Philosophy in Cognitive Neuroscience
Trieste, 2011

SISSA - Via Bonomea 265 - 34136 TRIESTE - ITALY

Acknowledgements

I want to thank Mathew E. Diamond. Without his constant support and fruitful discussion this work would have never been done.

I am grateful to Pavel Itskov, Ekaterina Vinnik, Arash Fassihi, and Yang Fang Zuo for their ideas, criticism and valuable comments to this work.

I am especially thankful to Athena Akrami and Federico Stella, for their substantial contribution to the experiments and data analysis and their willingness to discuss results.

Fabrizio Manzino, Igor Perkon, Marco Gigante and Stefano Parusso provided outstanding technical help apart from transmitting their enthusiasm and good spirit, making the work much easier. I'm grateful to them.

I dedicate this work to my lovely family; Marco and Camila.

Index

Abstract

Increasing amounts of work have demonstrated that brain rhythms might constitute clocking mechanisms against which to coordinate sequences of neural firing; such rhythms may be essential to the coding operations performed by the local networks. The sequence of operations underlying a tactile discrimination task in rats requires the animal to integrate two streams of information, those coming from the environment and, from reference memory the rules that dictate the correct response. The current study is a follow up on the work which has described the hippocampal representation of the tactile guided task. We have used a well-established texture discrimination task, in which rats have to associate two stimuli with two different reward locations. We placed microelectrodes in primary somatosensory cortex and the CA1 region of hippocampus to perform recordings of spiking activity and local field potentials when the animal touched the discriminandum as well as when he was in a resting state. We also performed recording on an arena in which the animal moved freely and did not perform any task. Earlier work has demonstrated that tactile signals reach the hippocampus during texture discrimination, presumably through the somatosensory cortex. We predicted that neurons in the primary somatosensory cortex (S1) are entrained to the oscillatory theta rhythm that permeates the hippocampus. Our expectation is that such coherence could serve to increase the reliability of synaptic transmission, linking the acquisition of new sensory information with associative processes. We addressed the following issues: Is the timing of action potentials in S1 modulated by the ongoing hippocampal theta rhythm? If so, is the occurrence of this modulation aligned in time to the period in which the hippocampus acquires tactile signals? We also predicted that the 10-Hz whisking that characterizes the acquisition of texture information would be more strongly phase locked to theta rhythm than the whisking in the air that is not accompanied by any explicit tactile task,. We speculate that such phase locking could be a means to synchronize sensory and hippocampal processing. The notion that the coordination between brain areas might be related to the rhythmic of sensorimotor cycles is particularly appealing. We have found that the firing of 18% of barrel cells was significantly modulated by hippocampal theta during the half-second period of active tactile discrimination. Importantly, we found that during periods of rest interleaved in the session, neurons significantly decreased the degree of phase-locking with respect to touch. We hypothesize that areas involved with motivational processes as basal ganglia could gate the entrainment during task related epochs.

S1 neurons were classified as those excited by contact with the discriminandum, and those not excited by contact. The firing of both sorts of neurons was modulated by CA1 theta rhythm

during exploration of the texture. However the theta phase to which they fired preferentially was opposite; contact-responsive neurons tended to fire in the upward phases of the cycle whereas contact non-responsive neurons tended to fire in the downward phase of the cycle suggesting that theta rhythm might have the function of temporally separating sensory cortical neurons according to their functional properties and the information they carry. By clustering touch-sensitive neurons to a certain time window and separating them from 'non-informative' neurons, theta rhythm could increase the efficiency not only of information tranfer to hippocampus but also the efficiency of information encoding/decoding.

We also found phase and amplitude relationships between whisking and hippocampal theta during the goal-directed tactile task; the relationships disappear when the animal moves along an open arena, still actively whisking but not engaged in the texture discrimination task.

We were able to show, for the first time to our knowledge, that CA1 theta rhythm can exert a behavioral state-dependent modulatory effect on sensory cortex. S1 neuron firing and whisking activity are entrained to hippocampal theta rhythm when the animal collects meaningful tactile information from the environment.

List of abbreviations

BG- basal ganglia

CA(1-3) - cornu ammonis subfields of hippocampus 1 to 3 respectively

DG- dentate gyrus (fascia dentata of hippocampus)

EC - entorhinal cortex

LEA- lateral entorhinal area

LFP- local field potential

LTP- long term potentiation

MCx- motor cortex

MEA- medial entorhinal area

NAc- Nucleus Accumbens

PL- lateral parietal cortex

PM - medial Parietal cortex

PoM - posteromedial complex of the thalamus

POR- postrhinal area

PTLp - posterior parietal cortex

PV - parietal ventral area (the same as S3)

S1- primary somatosensory cortex

S2 - secondary somatoseonsory cortex

S3 - tertiary somatosensory cortex

SN- substantia nigra

STDP- spike-timing dependent plasticity

TG-Trigeminal ganglion

TN- Trigeminal nuclei

VPM - posteromedial nucleus of the thalamus

VTA- ventral tegmental area

ZI- Zona Incerta (Ventral Thalamus)

Chapter I

Introduction

INTRODUCTION

Although brain oscillations have been observed for several decades, the development of new electrophysiological techniques, has led to a fundamental paradigm shift where the brain seen as a passive device turned to be regarded as a system with its own dynamics, which is perturbed by external influences. Accordingly, in the last 20 years there was a shift towards explaining cognitive functions in terms of the coherent behaviour of large neuronal populations that are dynamically bound within and across subsystems. Increasing amount of works have demonstrated that brain rhythms constitute clocking mechanisms against which to reference and coordinate sequence of neural firing and are essential to the specific coding operations performed by the various local networks in the brain.

Consider for instance, a tactile discrimination task where a rat has to touch different textures, and turn right or left according to the contacted texture in order to receive water. The sequence of cognitive processes behind the motor action requires not only a number of distinct brain regions, but also different sub networks within the same region. Each of these networks operates on the input it receives and feeds its output in turn; therefore it is clear that coordinated sequence and timing is critical for a coherent behavioral output. Given that the animal has to integrate two streams of information, those coming from the environment and, from reference memory the rules that dictate the correct response, the importance of this issue is that entraining of somatosensory neurons to an oscillatory rhythm as hippocampal theta range could increase the reliability of synaptic transmission, linking the acquisition of new sensory information with associative processes. Moreover, as synchronous oscillations would be particularly important in top-down modulation (Engel AK, Fries P and Singer W, 2001), the study of somatosensory processing in the context of attention and memory paradigms is a valuable approach to the highlighting of pioneering theories.

While there are no known rhythmic processes entraining the acquisition of visual information, the somatosensory system of rats stands out by the fact that information collection is cyclical. As will be described below, rats protract and retract their whiskers (“whisking”) in a rhythmic 10-Hz pattern. The notion that the coordination between brain areas might be related to the rhythmic of sensorimotor cycles is particularly appealing.

The current study is a follow up on the work which has described the hippocampal representation of the tactile guided task (Itskov PM, Vinnik E and Diamond ME, 2011) taking the main line of research of our laboratory devoted to unravel the neural coding mechanism of

somatosensory information (Arabzadeh E, Zorzin E and Diamond ME, 2005). To study the potential dynamical coupling between brain regions, we have used a well-established experimental paradigm: the two-texture discrimination task in which rats have to associate two different stimuli with two different reward locations (von Heimendahl M, Itskov PM, Arabzadeh E and Diamond ME, 2007). By placing microelectrodes in the regions of interest with a relatively simple surgical procedure, we were able to do stable recordings of the brain activity under different conditions.

Whiskers and Somatosensory Processing

Since rats are nocturnal animals living in tunnels and caves, the whisker system is likely to have evolved to be able to extract environmental information more accurately than what visual system could give. Perhaps the most remarkable specialization of this sensory system is the primary somatosensory cortex: the "barrel" cortex, where each whisker is represented by a discrete and well-defined structured in layer 4 (Woolsey TA and Van der Loos H, 1970). These layer IV barrels are somatotopically arranged in an almost identical way as the layout of the whisker on the snout. They form early in the development and therefore, the functional organization, and experience-dependent plasticity can be examined in the context of an invariant anatomical map.

Connectivity within the sensorimotor network

As rats are able to extract information by actively moving their vibrissae, tactile exploration entails the interplay between motor output and sensory input. This implies that there is a neuronal circuitry involved with vibrissae- mediated sensation and the control of vibrissae movement. These closed-loops (Kleinfeld D, Berg RW and O'Connor SM, 1999) (Kleinfeld D, Ahissar E and Diamond ME, 2006) are nested, and process sensory input from vibrissae and send projections to direct vibrissae movement. Five close-loops can be described, the hindbrain-loop confined to the ipsilateral side of the brain, and the high-order loops: midbrain-loop, cerebellar-loop, thalamic-loop and cortico-thalamic-loop that involve connections that cross midline. The vibrissae angular position is controlled by the follicles in the mystatial pad. Each follicle is innervated by neurons from the trigeminal sensory ganglion (TG), while motion of the follicles is under control of intrinsic and extrinsic mystatial muscles, both of which receive input from the facial motor nucleus (Dorfl J, 1982) (Dorfl J, 1985). These sensory and motor structures are linked via the trigeminal nuclei (TN) and form the hindbrain- loop. The hindbrain loop is nested within the midbrain-loop: superior colliculus has afferents from the TN and send descending projections to facial nucleus. Cerebellar-loop encompasses the former loops: the pontine- and olivocerebellar nuclei integrate input from the

TN, as well as superior colliculus who send back projections to facial nucleus. Multiple structures in ventral and dorsal thalamus receive input from the trigeminal nuclei. Only one of these, zona incerta (ZI) in the ventral thalamus, projects directly back to the superior colliculus forming the thalamic-loop. The highest level feedback loop in the vibrissa sensorimotor system involves multiple thalamic nuclei and cortical areas. Sensory projections from the trigeminal nuclei (TN) travel up through dorsal thalamus to primary sensory (S1) and motor areas of cortex (MCx). These two cotical areas send back projections directly to both the colliculus and reticular nuclei (Miyashita E, Keller A and Asanuma H, 1994) to close the loop.

Sensory Processing

In terms of whisker related sensory information the most important pathway regards the structures at the level of the forebrain (Diamond ME, von Heimendahl M, Magne Knutsen P, Kleinfeld D and Ahissar E, 2008) (Petersen CCH, 2007), the thalamic-loop and cortico-thalamic-loop. As explained above, sensory neurons make excitatory glutamatergic synapses in TN of the brain stem. From TN, three parallel afferent pathways reach thalamus and then S1: lemniscal, extralemniscal and paralemniscal pathways. In the lemniscal pathway, neurons from principal TN are organized into somatotopically arranged "barrelettes", each receiving strong input from a single whisker, reach ventral posterior medial (VPMdm) nucleus of the thalamus which is arranged into anatomical units termed "barreloids". Axons from VPMdm neurons within individual barreloids project to the primary somatosensory cortex forming discrete clusters in layer IV, which forms the basis of the barrel map. In the extralemniscal pathway, neurons in the caudal part of the interpolar TN are also clustered into whisker-related barrelettes. They project to the ventrolateral domain of the VPM (VPMvl), where neurons are clustered, and axons of this area project to the septa between the barrels of S1 and to the secondary somatosensory cortex (S2). Finally in the paralemniscal pathway, neurons from the rostral part of the interpolar TN are not spatially arranged. They project, among other targets to the medial part of the posterior nucleus (POm) of the dorsal thalamus and to the ZI from ventral thalamus. Axons from POm reach layers 5 of S1 and S2 and to the primary MCx. Even though function of the different pathways have not yet been directly tested and different groups have different hypothesis, numerous researchers (Diamond ME, von Heimendahl M, Magne Knutsen P, Kleinfeld D and Ahissar E, 2008) suggest that paralemniscal pathway in the POm would convey information about whisking kinematics, extralemniscal neurons in the VPMvl would code contact timing, while lemniscal neurons in the VPMdm would code detailed whisking and touch information.

Hippocampus

Neuroanatomy of the Hippocampus

During the phylogenetic development of mammals, topographic changes in the position of the hippocampus occurred. Hypotheses about the main cause of these changes point to the extensive development in some phyla of the neocortex and of the corpus callosum. Despite the 'migration' of the hippocampus, the architecture was remained stable across mammals. The following circuitry description applies to primate and non-primates mammals.

The hippocampal formation consists of hippocampus proper (Cornu Ammonis and Fascia Dentata), enthorinal cortex (EC) and subicular complex (Witter MP, Wouterlood FG, Naber PA and Van Haeften T, 2000). Hippocampus proper (we refer to it later as simply hippocampus) receives sensory input from EC via the trisynaptic and monosynaptic pathways. The trisynaptic pathway starts in layer 2 neurons of EC and terminates in the outer and middle molecular layer of the dentate gyrus (DG) and on CA3 neurons. DG sends mossy fibers to CA3; instead, CA3 sends Shaffer collaterals recurrently to itself and to CA1. CA1 projects to subiculum and subiculum returns the signal to the deep layers of EC. The monosynaptic pathway is a shortcut projection from layer 3 neurons of the EC to CA1 and subiculum (Witter MP and Amaral DG, 1991). Apart from above mentioned connections, it has been shown that perirhinal cortex has direct projections to subiculum and a part of CA1 (Naber PA, Witter MP and Lopes Silva FH, 2001). As a result the structure of connections between EC and hippocampus can be described as a combination of sequential and parallel loops (via trisynaptic pathway with multiple shortcuts directly connecting EC with each of the hippocampal subfields and subiculum). EC has connections which link deep and superficial layers (Witter MP and Moser EI, 2006).

Three well-known properties of hippocampal circuitry can be described: 1) Hippocampus receives convergent afferents from virtually all cortical association and sensory areas, and these inputs are widely distributed in to the cell population of the different subdivisions. 2) principal neurons of CA3 send considerable projections to other CA3 cell, and these recurrent connections are sparse and mainly excitatory glutamatergic synapses. 3) The hippocampus is noted for the prevalence of rapid synaptic plasticity, known as long term potentiation or LTP (Bliss TVP and Collingridge GL, 1993) a process linked to memory formation.

Functions of the Hippocampus

Research on the hippocampus can be subdivided into two different bodies of experiments with different approaches motivated by largely different hypothesis about hippocampal function. Associated for a long time with the formation of episodic and semantic memories, the hippocampus is also regarded as a structure involved in spatial navigation. The idea that the hippocampus is a region devoted to memory functions comes from the systematic clinical documentation of the effects on memory of the resection of the temporal lobe (the most famous case is the patient H.M. reported 50 years ago), whereas the second line comes from discovery, in 1971, of place cells (O'Keefe J and Dostrovsky J., 1971) in rats. These two independent perspectives are not necessarily exclusive; indeed they have coexisted for the last 40 years, making major advances on their own directions. Still, many efforts were put forward to make them fit into the same conceptual paradigm (but see (Stella F, Cerasti E, Si B, Jezek K and Treves A, 2011) submitted for a perspective opinion on this issue.

Place cells are neurons that fire according to the animal's location within the environment. Different neurons are active in different places, so that the environment is represented by the entire population. Place cells undergo 'remapping' when the environment changes. Place cells gave rise to the cognitive map theory postulates that hippocampus is crucial in the formation of a navigational map of the environment (O'Keefe J, Nadel L, 1978). But, their activity has been shown to be related not only to the spatial location but also to a large number of other variables: they can also represent future locations (Frank LM, Brown EN and Wilson M, 2000), past locations (Ferbinteanu J and Shapiro ML, 2003), intended locations (Johnson A and Redish AD, 2007), and trajectories (Ji D and Wilson MA., 2008). Also these cells have the ability to recapitulate acquired experience during slow wave sleep (Lee AK and Wilson MA, 2006), REM sleep (Louie K and Wilson MA, 2001). On the other hand, apart from spatially related firing, many non-spatial factors have been shown to affect firing of hippocampal neurons. Among such factors were different odors, conjunctions between odors and places (Wood ER, Dudchenko PA, Robitsek RJ and Eichenbaum H., 2000), sounds (Moita MA, Rosis S, Zhou Y, LeDoux JE and Blair HT, 2004) among others. These intriguing features of place cells posed the question of whether space coding is simply the frame within which more complex memories are constructed. Indeed this gave rise to hybrid theories between navigational map and the relational theories exposed below (Leutgeb S, Leutgeb JK, Barnes CA, Moser EI and McNaughton BL, 2005).

In parallel to the place cell evidence, the role in memory processing given the clinical and experimental evidence, together with the circuitry features (convergent inputs, strong recurrency

and rapid LTP) gave rise three major qualitative models of hippocampal function: the 'standard model' (Squire L and Zola-Morgan S, 1991), and later the 'memory trace model' (Nadel L and Moscovitch M, 1997) (Nadel L, Samsonovich A, Ryan L and Moscovitch M, 2000) and finally binding model (Wallenstein GV, Eichenbaum H and Hasselmo ME, 1998). The standard model, a reinterpretation of Marr's theory (Marr D, 1971), states that the hippocampus binds or associates cortical representations that are active by making the inputs converge into its structure. The binding increases the probability that such representation will be activated later in time. Such reactivation triggers a slower consolidation process between cortico-cortical interconnections and once this is completed, long term memories are no longer dependent on the medial temporal lobe. As this model does not differentiate between episodic and semantic memory, it cannot account for the different pattern of amnesia for episodic and semantic memory. Nadel et al (2000) therefore proposed an alternative model. The 'multiple trace model' states that hippocampus is always involved in the storage and retrieval of episodic memories independent of their age. Although experience is initially encoded in distributed hippocampo-cortical networks, the hippocampus is always required for rich contextual or spatial detail; a feature of episodic memory. So each experience leads to the generation of a separate memory trace in the hippocampus, but also each retrieval of a memory trace leads to the regeneration of a new episodic trace in hippocampus, which share some or all information about the initial episode. The creation of multiple related traces facilitates the extraction of factual information giving rise to the formation of semantic memories. In the third model, Wallenstein et al followed the same rational as the previous models but stressed experimental evidence on rats and with a more computational perspective: they argued that this structure is involved most critically in learning and memory tasks in which discontiguous items must be associated, in terms of their temporal or spatial positioning, or both.

An interesting aspect of this proposal is that it fits with the place cell perspective together with the neurophysiological data. As outlined above, the place cell representation could be used as a scaffold, providing the spatio-temporal context to the episodic memories (Eichenbaum H, Dudchenko P, Wood E, Shapiro M and Tanila, H, 1999) (Eichenbaum H, 2000b)

Oscillations

If we place low impedance microelectrodes in the extracellular environment we measure voltage changes with respect to a reference. These voltage changes are small charge imbalances across the cell membrane and are generated by currents flowing across the membrane. These currents arise both from action potentials and from synaptic activity. Correspondingly, the voltages

recorded with microelectrodes typically contain two kinds of activity: spikes with high frequency content (order of milliseconds), and the so-called "local field potential" (LFP) with lower frequency content. The LFP signal reflects neurons assembly behaviour and is characterized by its oscillatory property (Pedemonte M, Velluti RA, 2005) (Hyman JM, Zilli EA, Paley AM, and Hasselmo ME, 2005) (Engel AK, Fries P and Singer W, 2001). The origin of the LFP is complex and continues to be subject of research. The LFP is composed mostly of sustained slow currents like excitatory postsynaptic potentials (EPSPs) and inhibitory postsynaptic potentials (IPSPs) (Mitzdorf U, 1985) (Kamondi A, Acsády L, Wang XJ and Buzsáki G, 1998), but also of unrelated synaptic events like spike after-potentials and voltage-dependent membrane oscillations. In this way, the synchronized and periodic sub-threshold potential changes of a cell assembly emerge from the dynamic interplay between intrinsic cellular and circuit properties (Gray CM & McCormick DA, 1996). At the single cell level, certain neurons intrinsically resonate, a phenomenon generated by interactions between calcium- and voltage-dependent channels. At the network level, the genesis of oscillations, their initiation, propagation, termination, and large-scale synchrony emerge from interactions between neurons with a variety of intrinsic cellular properties through different types of synaptic receptors.

Neuronal networks in the mammalian forebrain as well as cortex demonstrate several oscillatory bands covering frequencies from approximately 0.05 Hz to 500 Hz (Buzsaki G, 2006) The mean frequencies of the experimentally observed oscillator categories form a linear progression on a natural logarithmic scale (Penttonen M, Buzsaki G, 2003) with a constant ratio between neighbouring frequencies, leading to the separation of frequency bands. Neighbouring frequency bands within the same neuronal network are typically associated with different brain states and compete with each other (Bragin A, Jando G, Nadasdy Z, Hetke J, Wise K and Buzsaki G , 1995). On the other hand, several rhythms can temporally coexist in the same or different structures and interact with each other (Csicsvari J, Jamieson B, Wise KD, Buzsaki G, 2003)

Theta rhythm in hippocampus

The hippocampal 5-12Hz band oscillation, called Theta rhythm, is the most prominent rhythm of the forebrain (Buzsaki, 2006). According to different studies, several rhythm generating mechanisms and numerous current dipoles are part of a dynamic consortium. Indeed the idea that the medial septum functions as a temporal coordinator of hippocampal networks (Lee MG, Chrobak JJ, Sik A, Wiley RG, Buzsaki G , 1994) has faded with the discovery of a much more complex scenario: each anatomical layer of the hippocampus has its own theta current dipole, and this can vary somewhat independently from one another. More precisely, it was shown that layer-specific fluctuations in power, coherence and phase accompany different cognitive states of the animal

(Montgomery SM, Betancur MI and Buzsaki G, 2009), and although the activities of different dipoles are interrelated, dipole combinations may be used to support flexible processing within the global theta system.

The role of Theta Rhythm

Dynamic coupling of different brain regions and the role of Theta oscillations

As we mentioned before, oscillations are a key mechanism for dynamical coupling between brain areas. Task and state dependent changes are observed in local field potential coherence. Jones MW and Wilson M (Jones MW and Wilson M, 2005) were able to explicitly relate variations in phase-locking of neurons with variations in behavioral demands. They showed that correlated firing in mPFC and hippocampus is selectively enhanced during spatial working memory epochs, and this increase is paralleled by enhanced coupling of the two structures in the 4- to 12-Hz theta-frequency range. In line with this study, Hyman et al (Frontiers in Integrative Neuroscience 2010) showed only theta-entrainment was correlated with successful memory performance, indicating mPFC-HPC theta-range interactions are the key to successful DNMS performance.

Temporal relation of Neurons activity in a network and the role of Theta oscillations

With regards to its function within areas, Singer W. in 1993 (Artola A and Singer W, 1993) suggested that single synapses are modified according to the temporal relations of the electrical activity of the neurons in a network and in 1997, Markram H. et al (Markram H, Lübke J, Frotscher M and Sakmann B, 1997) showed that correlated spike times is critical for spike-timing dependent plasticity (STDP). In a recent work, Benchenane K. *et al* (Benchenane K, Peyrache A, Khamassi M, Tierney PL, Gioanni Y, Battaglia FP and Wiener SI, 2010) found that 1) coherence between hippocampus and PFC increased with learning of the contingency rule, and that 2) synchronous PFC cell assemblies emerged simultaneously; a phenomenon replicated with the application in anesthetized animals of dopamine; a neuromodulator that signals reward expectation. Moreover, they showed that cell assemblies emerging during high coherence were preferentially replayed during subsequent sleep. Thus, this study not only shows that theta oscillations are used for coordination of both regions activity, but also suggests that their activity has an active role in synaptic learning and consolidation of memory traces, and so, that they are essential to the specific operations performed by the distant network synchronized, linking together both perspective on the role of the theta system.

Top-down concept in light of oscillations

Contrasting classical theories of sensory processing where the brain is a passive stimulus-driven device, Singer W et al suggested that top–down influences such as memory, attention or expectation of forthcoming events strongly shape the intrinsic dynamics of thalamocortical networks. These top-down influences refer to the fact that many aspects of cognition and behaviour are not stimulus driven in a reflex-like manner, but are to a large degree based on expectations derived from previous experience, and on generalized knowledge stored in the architecture of cortical and sub- cortical networks. Accordingly, they proposed that synchronous oscillations are particularly important in this process (Engel AK, Fries P and Singer W. , 2001), building in this way a more complete scenario on the role of oscillations in the brain. In this sense, the study of hippocampal oscillations in terms of driving perceptual information would be highlighting.

Linking S1 to Hippocampus (and the rest of the brain)

Somatosensory Input to the Hippocampal formation

Sensory information arrives in the temporal lobe through both unimodal and multimodal cortical sensory areas. Information about individual stimuli originates in unimodal sensory areas (like S1) forwarded to the hippocampus through the perirhinal cortex and lateral entorhinal area (Burwell RD and Amaral DG., 1998). Contextual information related to the spatial arrangement of distinct objects, in contrast, reaches the hippocampus through the parahippocampal cortex and medial entorhinal area. From the entorhinal area, where both pathways converge, sensory stimuli reach the hippocampus through the perforant path, which targets the CA1 and CA3 fields. Pereira et al (Pereira A, Ribeiro S, Wiest M, Moore LC, Pantoja J, Lin S and Nicolelis MA, 2007) investigated how whiskers reach CA1. Using simultaneous recording and chemical inactivation in behaving rats, they showed that trigeminal inputs from whiskers reach the CA1 region through thalamic and cortical relays, more specifically through the lemniscal pathway.

The "what" pathway: Hippocampal representation of tactile guided task

Experiments carried out in our laboratory (Itskov PM, Vinnik E and Diamond ME, 2011) provided a characterization of tactile encoding in rat hippocampus in a three-texture and four-texture discrimination paradigm which allowed the investigators to disentangle texture from reward

location information. It was shown that neurons from CA1 form a texture representation independently of the action the stimulus is associated with. But, unlike the texture representation in barrel cortex, the representation in hippocampus did not reflect the physical properties of the stimulus. Neurons did not encode textured stimuli as physical objects along the dimension of coarseness, but as meaningful events in conjunction with the location in which they appeared. Moreover, neuronal information (contrary to single cell activity) about the palpated texture did not disappear when the whiskers broke off contact with the discriminandum as occurs in early stages of sensory processing, but persisted and even showed a slight increase in strength one-half second after reward onset. In these experiments, the conjunctions between texture and reward location signal are consistent with the binding theory (Wallenstein GV, Eichenbaum H and Hasselmo ME, 1998), whereas the strong influence of the animal's location on neuronal firing is consistent the cognitive map theory. From a computational perspective the early input might be "stretched" in time to be made contiguous and matched with a later input (reward location or action), ultimately allowing phenomena of synaptic plasticity to take part in the consolidation/reconsolidation of the associative memory.

Sirota et al (Neuron (Sirota A, Montgomery S, Fujisawa S, Isomura Y, Zugaro M and Buzsáki G, 2008) recorded unit activity and local field potentials (LFP) from multiple neocortical regions, including primary somatosensory area (trunk representation) along with hippocampal activity in rats and mice that were not performing any specific cognitive task (some of them were performing a working memory task, others were sleeping, REM phase). They reported that a significant fraction of neurons in all recorded neocortical areas are phase modulated by the hippocampal theta rhythm. Importantly, theta-modulated neurons were found not only in the PFC which has massive direct afferents from the hippocampus, but also in the primary somatosensory area, which has only multisynaptic connections with the hippocampus (Witter MP, Wouterlood FG, Naber PA and Van Haeften T, 2000; Witter MP, 1993).

Kleinfeld et al (Berg RW, Whitmer D and Kleinfeld D, 2006) revisited the issue of coherence between whisking and hippocampal theta rhythm. They found that the fraction of epochs with high coherence was not significantly greater than that expected by chance. They further observed that the strength of theta rhythm did not correlate with that of whisking. But they tested this hypothesis in rats trained to whisk in the air, without any goal and reward. As they pointed out in the paper, and considering its previous work, "phase relationship between whisking and the theta rhythm may well depend on the state of the animal". Thus it is possible that the theta rhythm and whisking will phase lock when the animal learns to discriminate an object (or surface) with the

vibrissae, a prediction consistent with the increasing evidence that synchronized activity between brain areas emerges under certain cognitive demands (or behavioral states) and behavioral context.

In light of these last experiments, the present study was conceived to address the following emerging questions: does hippocampal theta exerts its modulation several synapses away as primary sensory areas? Is this modulation of the firing restricted to specific behavioral states of the animal? We also asked whether goal directed whisking in contrast to air whisking is phase locked to theta rhythm as a means to synchronize sensory and hippocampal processing.

Chapter II

General Methodology

Subjects

Wistar male rats (Harlan Italy, S. Pietro al Natisone, Italy) weighing about 300 g were housed in pairs and maintained on a 12/12-h dark/light cycle till the moment of surgery. Rats were habituated to the researcher (handling procedure) for five days before the experiments started. All experiments were conducted during the dark phase. Food was ad libitum throughout the experiment. Water was given during training as a reward and was also available ad lib for 10 min after training. All experiments were conducted in accordance with National Institutes of Health, international, and institutional standards for the care and use of animals in research and were supervised by a consulting veterinarian.

Experimental set-up

Discrimination Task:

Rats were trained to perform a tactile discrimination task 1) a two textures scheme (pseudorandom presentation): two or three rectangular plexiglass with different surface were associated with two opposite reward places (see *Discriminanda*). Set-up (Figure 1a) consisted on a 10cmx30cm elevated platform with two front lateral water spouts, a movable bridge and a front central motor. Hi-speed camera (1000fps-512 X 512 pixels, (Optronis CamRecord 450, Optronis)) was positioned on top in order to capture whisker movements and touch contact during the task (Figure 1b). Central and lateral light sensors were used to synchronize behavior with electrophysiological recordings and hi-speed films. All set up was commanded with Labview software (National Instruments Co).

Discriminanda

Two different sets of discriminanda were used (Figure 2). First set consisted on one sandpaper texture plexiglass rectangle and a smooth texture plexiglass rectangle. The second set on three plexiglass rectangles: two with vertical grooves (2mm and 4 mm length) and one smooth.

In the case of three texture discrimination task vertical grooves (2 mm and 4mm apart) were associated with reward on the right side and smooth surface with reward to the left side.

a)

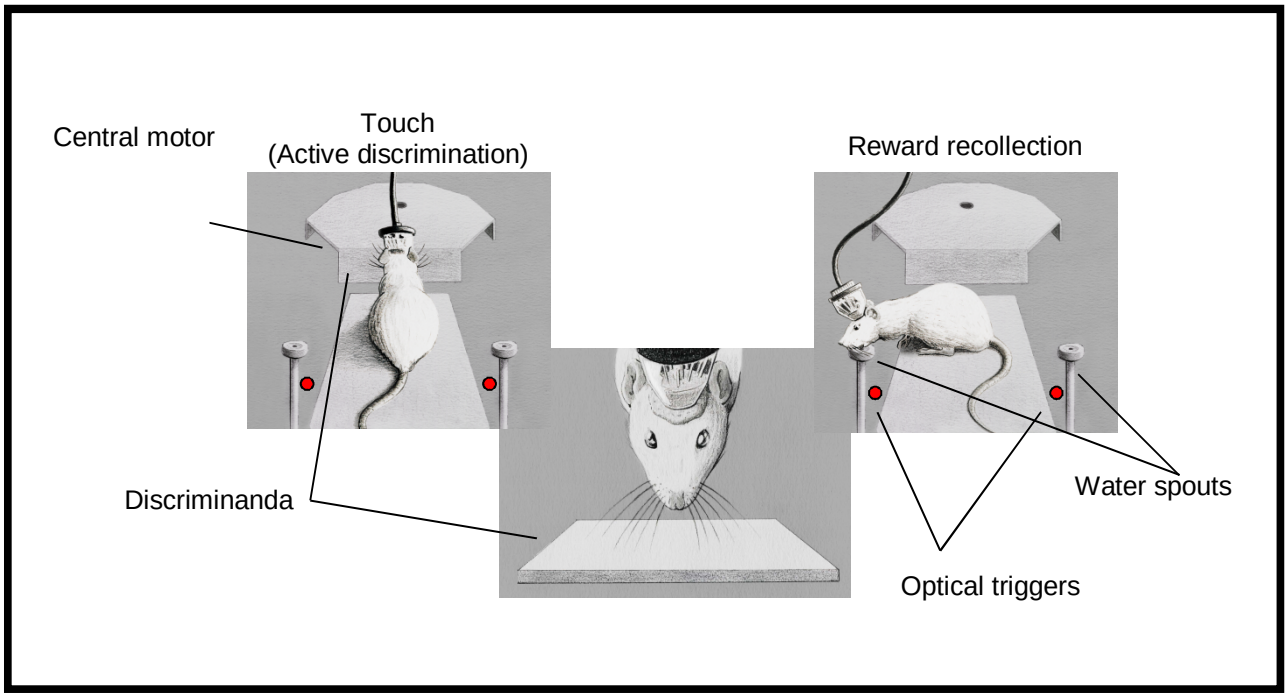

b)

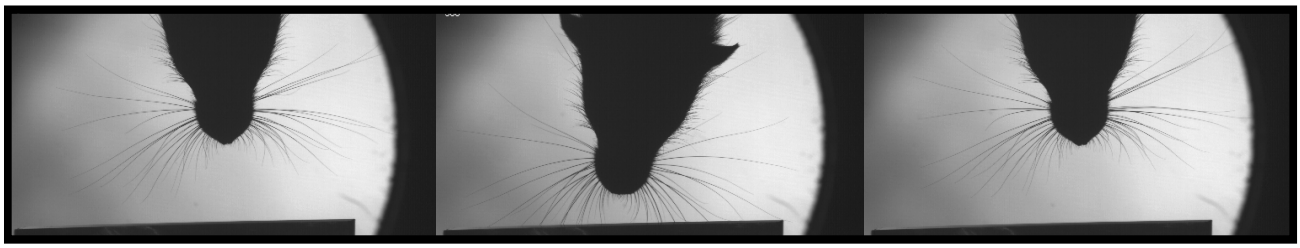

Figure 1: Discrimination Task. a) Two or three different textures were associated with two opposite reward places. Central and lateral light sensors were used to synchronize behaviour with electrophysiological recordings and hi-speed films. b) Hi-speed camera (1000fps) was positioned on top in order to capture whisker movements and touch contact during the task.

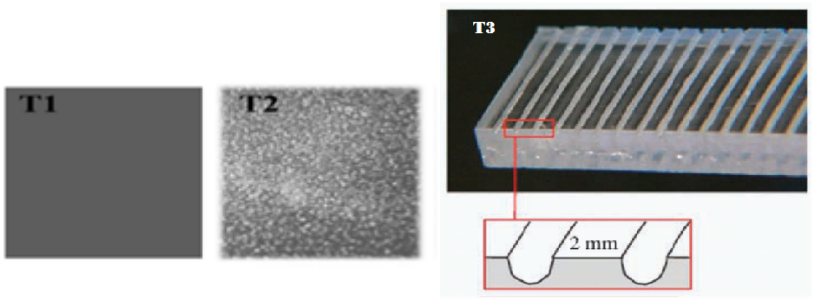

Figure 2: Discriminanda. Set of sandpaper and groove textures. T1: smooth, T2: rough.T3: 2mm groove

Free moving Arena:

Rats were also trained to whisk on the air on while walking back and forward on a squared platform (Figure 3). (40cmx40cm) in which cereals scales were delivered randomly (see picture) Hi-speed camera (200fps- 800×600, and smooth surface) was positioned on top in order to capture whiskers motion. For details see Chapter IV, Materials and Methods.

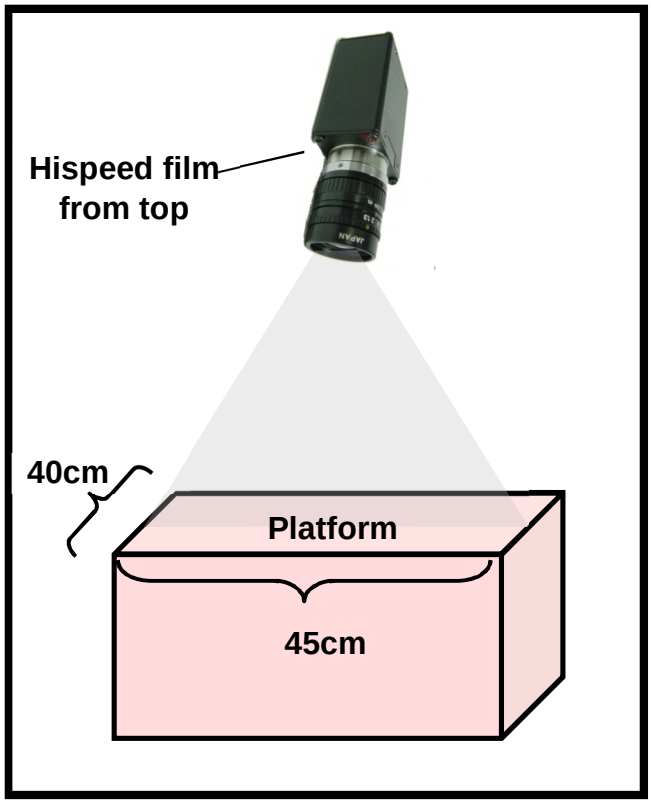

Figure 3: Free Moving Arena.

Surgery

Once animals reached stable performance (>80% correct trials), surgery for tetrodes implantation was done. Animals were anaesthetized with a mixture of Zoletil (30 mg/kg) and Xylazine (5 mg/kg) delivered intraperitoneally. Small screws were fixed in the skull as a support for dental cement. One of the screws served as a ground electrode. A craniotomy was then made over hippocampus and barrel cortex, centred 2.76 mm posterior to bregma and 3 mm lateral to the midline (Paxinos). Dura mater was removed and exposed tissue was covered with biocompatible silicon (KwikSil; World Precision Instruments). A twelve-tetrode microdrive (Neuralynx) was positioned with micromanipulator (Hippocampus bundle:-3mm AP, -2mm L. S1 bundle: -2.7mm AP, 5.5mm L) above the craniotomy and attached by phosphate dental cement. Rats were given the

antibiotic enrofloxacin (Baytril; 5 mg/kg delivered through the water bottle) and the analgesic caprofen (Rimadyl; 2.5 mg/kg, subcutaneous injection) for a week after surgery. For 10 d after surgery, they had unlimited access to water and food. Recording sessions in the apparatus began thereafter.

Hyperdrive Design and tetrodes construction

A microdrive (Hyperdrive-Neuralynx) was loaded with 10-12 custom-made movable tetrodes (25 µm wire PI/Ir wire) (Fig 4). Two single bundles composed of stainless guide tubes 3.5mm apart (distance between dorsal Hippocampus and S1) guided 2-4 tetrodes to target CA1, and 8 tetrodes to target S1 central barrels (Fig 5)

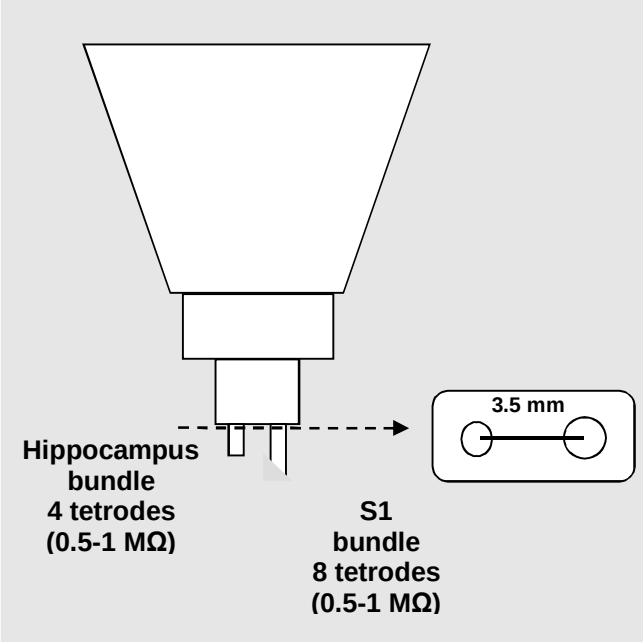

Figure 4: Microdrive Design (Neuralynx Hyperdrive 12 tetrodes)

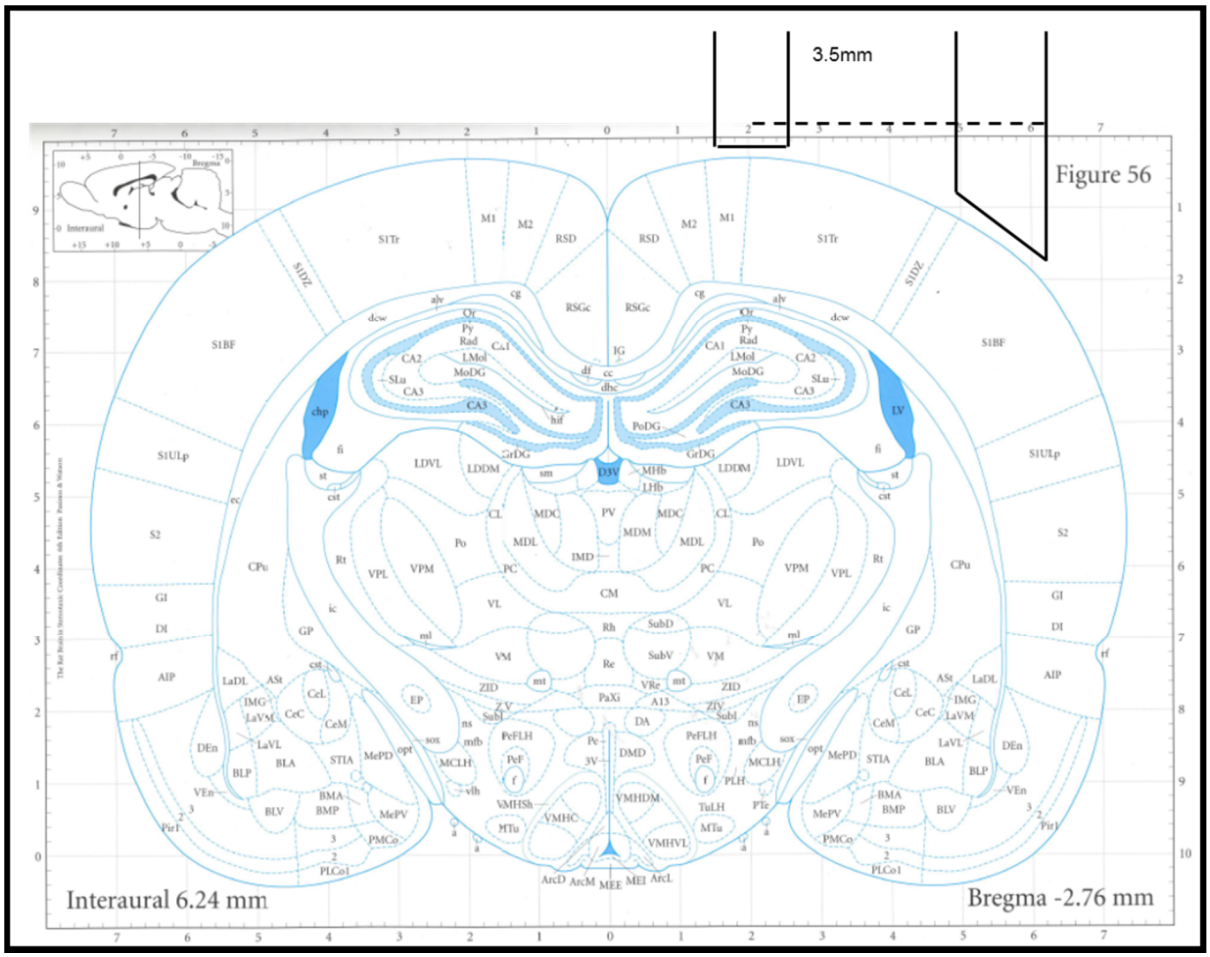

Figure 5: Bundles position according to Paxinos Atlas. Hippocampus bundle:-3mm AP, -2mm L. S1 bundle: -2.7mm AP, 5.5mm L.

Electrophysiological Recording and Data preprocessing

At a depth of about 900 um, it became possible to distinguish action potential waveforms evoked by manual whisker stimulation. Data reported here came from recordings at depth of 900-1100µm, i.e. layer IV. The spike signals were amplified by a factor of 1000–5000, bandpass filtered between 600 Hz and 6 kHz, and digitized at 32 kHz. Spikes were sorted offline on the basis of the amplitude and principal components by means of semiautomatic clustering algorithms (BBClust, written by P. Lipa, and KlustaKwik, written by K. D. Harris). The resulting classification was corrected and refined manually with MClust software (written by A. D. Redish). Single-unites were identified based on clear refractory period, otherwise they were considered multi-units. Electrodes position were frequently moved (one quarter of turn of the guiding screw is equivalent to 40um depth) in order to get different pool of neurons from session to session. Data

recorded in different sessions from the same electrode, were always analysed as separate clusters. Only neurons with constant signal throughout the session were included in the analysis

To measure Local Field Potentials (LFPs) from CA1 a copy of the signal from an electrode that was used for the recording of spikes was amplified by a factor of 1000-2000, band pass filtered between 1 Hz and 475 Hz, and digitized at 2 kHz. The reference electrode was the bundle of stainless guide Online visual inspection of prominent Theta waveforms in addition to histology confirmed the position of the tetrodes.

LFP Power Spectrum and Coherence

For power spectrum we used 1 taper (Hanning taper) applied to a 0.56 or 0.68 sec time length and frequency resolution 2Hz (Chapter IV experiments) and 2 tapers (Slepian tapers) to a 1.2sec-1Hz window before the Fourier transform (Chapter III experiments). Frequency range of analysis was 4-20Hz. The Fourier transform is a mathematical operation that decomposes a signal into its constituent frequencies. It is extensively used in signal processing and LFPs can be seen as a sequence of time points or time series. Such a time series can be described as the sum over sines and cosines of varying magnitudes, frequencies, and phases which can be also represented as sum of complex exponentials:

$$f(t)= e^{i\omega t} = cos(\omega t) + isin(\omega t),$$

with ω being the angular frequency related to the conventional frequency $\omega=2\pi f$

The (Discrete) Fourier Transform is defined by:

$$X_i(f) = \sum_{t}^{T} w(t)\, X_i(t) e^{-2\pi jft},$$

where $xi(t)$ is the time series of the LFP data segment and $w(t)$ the taper or window function. The window function is a mathematical function that is zero-valued outside of some chosen interval. When another function or signal is multiplied by a window function, the product is also zero-valued outside the interval. Tapers are used in signal processing to alleviate for spectral-leakage; an feature of finite-length signals or finite-length segments of infinite signals where it appears as if some energy has "leaked" out of the original signal spectrum into other frequencies. Non-rectangular window functions, i.e. tapering functions, actually increase the total leakage, but they can also redistribute it to places where it does the least harm, depending on the application. In this analysis we used Hanning window.

Power spectrum (S_i) is defined as,

$$S_i = | Xi(f) |^2$$

Standard error of power spectrum was computed by means of the Jackknife method. Jackknife method computes the variance of a power spectrum population drawn from sample population leaving one sample out. The rational of this non-parametric method is the following: in the absence of any other knowledge about the population the distribution found in a random sample of size n from the population is the best guide to the distribution in the population.

Test for significant differences in the Power Spectrum (and PLV) between conditions

We tested for significant differences between any conditions performing a Montecarlo test (Fieldtrip Toolbox). In this case the significance probabilities and/or critical values were calculated by building random partitions: we randomly drew as many trials from the combined data set as there were trials in condition 1 and place them into subset 1and the remaining trials are placed in subset 2. We calculated the t statistic (two sample ttest) for the random partition and repeated the procedure 1000 times building a histogram of the test statistic. From the test statistic that was actually observed and the histogram, we calculated the proportion of random partitions that were in a larger test statistic than the observed one. This proportion is the Monte Carlo significance probability, which is also called a *p-value*. We applied Bonferroni for multiple comparison correction.

Chapter III

Relationship between Barrel Cortex and Hippocampal Theta Rhythm

MATERIALS AND METHODS

See Chapter II (General Methodology) for Training procedure, Surgery and Recording.

Experiment

Discrimination Task

Five rats were trained to perform a tactile discrimination task 1) four rats were trained in a two textures scheme (pseudorandom presentation: each texture could be presented for three consecutive trials at most), 2) one rat was trained in a three texture scheme associated with two opposite reward places (2mm grooves and 4mm groove surface-to right reward and whereas surface smooth to left).

Behavioral Performance

Rat's performance of each recording session was tested statistically for being above chance by means of a randomization method. Texture labels were randomly shuffled across trials 500 times, and "performance" after each shuffle was calculated to get the distribution of percentage of correct trials. We compared the observed rat's performance to the shuffle distribution, and if its probability was $p<0.05$, then we concluded the animal made choices based on texture. For individual textures performance in each session we applied the same procedure. We computed the observed performance and the distribution of percentage of correct trials for shuffled data. With this method we controlled for choice bias.

Data PreProcessing

All analyses were performed using custom-written tools in Matlab (Mathworks) unless stated.

LFP Analysis

LFPs from Hippocampus were filtered between 5-12 Hz using a FIR filter (back and forward) with Kaiser window. After band-pass filtering of LFP in the theta range, instantaneous theta phase was estimated by Hilbert transformation. Distribution of phases in each session was tested for uniformity prior to unit analysis, and was corrected for the bias with a Ψ-transform

(Siapas AG, Lubenov EV and Wilson MA, 2005). This is a more conservative approach given that wave shape asymmetry depends on filter settings, instantaneous theta power and frequency and it varies in time.

Neurons Responsiveness Dynamics, Classification and Spike Phase assignment

Clusters from S1 were classified as 'Contact responsive' or 'Contact Non-responsive', by comparing its firing rate during Touch period and 3 sec before Trial started (Baseline period) with Paired t-test ($p<0.01$, Touch Time vs. Baseline). As theta signal was decomposed into instantaneous amplitude and phase components with Hilbert transformation, a spike occurring at time t was assigned phase value $\Phi(t)$. In this way the spike train of each cell was converted into a sequence of unit length vectors with an orientation given by the phase values of their corresponding spikes. In the discrimination task two period of time were extracted.

Periods of time taken for the analysis

As we mentioned before rats were trained in a pseudorandom scheme of two or three discriminanda with intertrial intervals (ITIs) of minimum 7 seconds. In all sessions as the training progressed and so the rat got more satiated, the rate of periods of rest (of 30 sec minimum) increased (confirmed by session films). This allowed us to extract periods of time were the rat was in a resting condition in the middle of the recording. In a first step for establishing criteria we observed (through random selection of session films/rats) that resting intervals were only present in the second half of the session. After that we did a systematic analysis: sessions were divided in quartiles and frequency of ITIs longer than 40 seconds was calculated, confirming visual inspection. So, ITIs longer than 40 sec corresponding to the second half of the session where taken for the analysis.

Spike-LFP Phase-Locking Analysis

Testing whether a neuron tends to spike in a certain phase of theta rhythm poses us in front of a problem of circular distribution. We will describe in this section the principal model of distribution against which our data was tested and the statistical tools applied. CircStat toolbox (Berens P, 2009) was used.

The von Mises Distribution

Under the hypothesis of rhythmic modulation of unit firing, neurons would tend to fire at a certain point of the period of the LFP. This pattern can be described as a von Mises distribution, with a mean direction in a cycle and a concentration parameter that reflects the degree of strength of such modulation.

The von Mises is a unimodal distribution with probability density function

$$.....f(\Phi|\,\theta,\,\kappa)=\frac{e^{\kappa\cos(\Phi-\theta)}}{2\pi I_0(\kappa)}$$

with parameters, κ ,θ (mean angle) and I_o (a modified Bessel function explained below). The function takes on its maximum value at $x = \theta$; hence θ is the mode. The distribution is symmetric with respect to the mode, therefore, θ is also the *mean angle*. The parameters θ and κ are analogous to the mean and variance in the linear normal distribution. For $\kappa=0$ the von Mises distribution degenerates into the uniform distribution;

$$.....f(x)= 1/2\pi$$

On the other hand, the larger the κ the more the distribution is concentrated around the mean direction. Therefore, κ is called the *parameter of concentration (Fig 1 a and b)*

a) *b)*

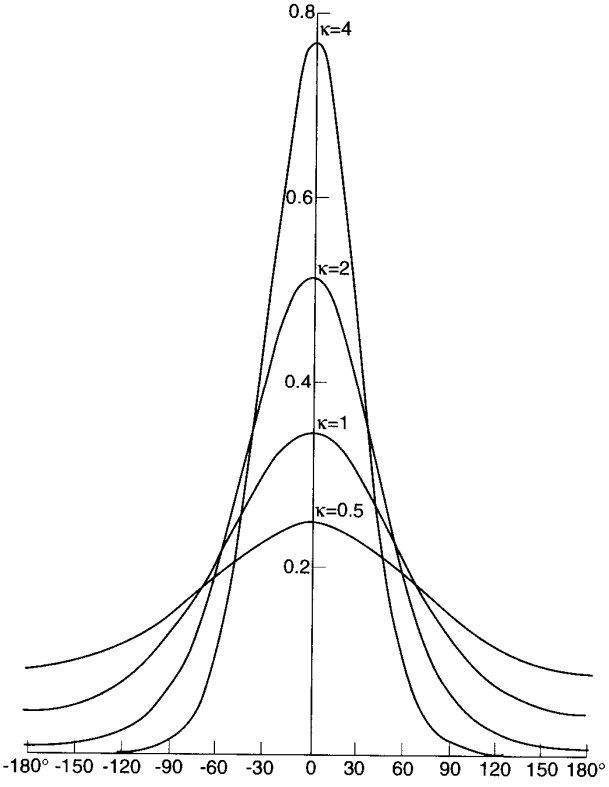

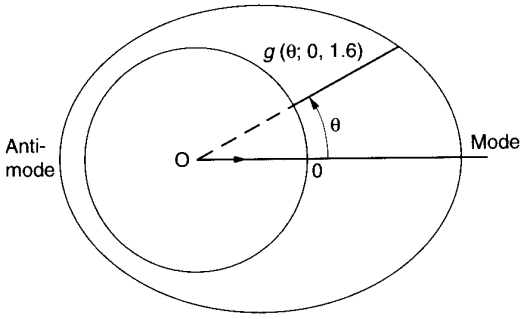

Figure 1: a) Density of the von Mises distribution M(0,κ) for k=0.5,1,2,4. b) Polar representation of the density g(0,1.6) of the von Mises distribution M(0,1.6).Taken from Batschelet (Circular Statistics in Biology, pages 37-38)

The centre of mass is given by the mean vector μ. Its polar vector θ, and its length is:

$$|\mu|=\rho= A(\kappa)$$

Being A(κ):

$$A(\kappa)= I_1(\kappa)/I_0(\kappa) \text{ with } \kappa >=0.$$

This function is monotonic increasing from the value A(0)=0 on. It reaches the value 1 asymptotically as κ tends to infinity. With the inverse function numerical values of κ can be extracted as a function of ρ: $\kappa= A^{-1}(\rho)$.

I_o and I_1 are modified Bessel functions. These functions belong to a family functions that solve problems in the circular, cylindrical and spherical coordinate systems. For details (Batschelet E, 1981) page 295-299 but also see (Mardia KV and Jupp PE, 2000) Appendix I, page 349.

Rayleigh Test

Rayleigh test is the most powerful invariant test of uniformity against the von Mises alternative. The basics are: given the sum of n vectors representing the preferred directions, it tests whether the mean length (r) is sufficiently large to indicate confidently a non-uniform distribution. Therefore, the appropriate statistics for significance test is:

$$Z = 1/n*(\Sigma \cos(\Phi_i)^2 + \Sigma \sin(\Phi_i)^2) \qquad \text{with } \Sigma \cos(\Phi_i)^2 + \Sigma \sin(\Phi_i)^2 = r$$

$$Z=2nr^2$$

or variance-stabilized *log(Z)*.It follows that the large-sample asymptotic distribution of Z under uniformity is χ^2 with two degrees of freedom (Mardia and Jupp, 2000, page 94-98).

Therefore it is intuitively reasonable to reject uniformity when Z (derived from vector sample mean) is far from 0. The alternative hypothesis is that population has von Mises distribution and this can be interpreted explaining the Rayleigh test as a likelihood ratio test of uniformity within the von Mises family. In such interpretation (formal explanation can be found in Mardia and Jupp, 2000, page 94), both competing models are fitted separately to the data and the log likelihood ratio is evaluated for its probability. Since the resultant score statistic is an increasing function of r the likelihood ratio test is equivalent to the Rayleigh test.

We notice that as mean vector length (r) depends on the sample size, all measures derived from r will depend on sample size (Figure 2). Indeed, the statistical distribution under the null hypothesis is only true asymptotically. For few data point, the null distribution of Z is typically broader, and therefore H_o harder to reject; whereas with more data points the distribution narrows, and if data really comes from H_a it is easier to establish.

Figure 2: Frequency distributions of the mean vector length, r, for samples of size N=10 and N=20 under the assumption that the directions are randomly distributed (uniform distribution). Although the theoretical mean vector is a zero vector, the sample mean vector ranges in length from 0 to 1. For N=10, r most frequently takes values between 0.1 and 0.4 with mode 0.23, whereas for N=20 the values are on average smaller. Thus, an increase in sample size results in a decrease of mean vector length, on the average over many samples. Taken from Batschelet (Circular Statistics in Biology, page 199)

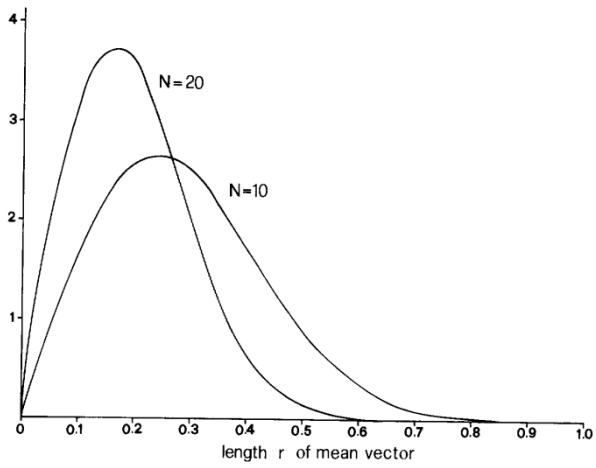

Sirota *et al* (2008) made the point on this issue, and after performing simulations they found, with regards to Rayleigh test performance for small samples, 'that p-values were in very close agreement for even very small sample sizes' (see Supplemental Data). But since they reported having computed "bootstrap Rayleigh tests by subsampling each sample 500 times with a subsample of size 100, in order to rule out the effect of sample size on the statistics at the cost of dramatically reducing power of the test for cells with high sample size", we decided to extend the study to better understand test performance and decide which criteria is more accurate. We performed Montecarlo simulations of von Mises populations with *k* less than 1 (as it is reported in Sirota A *et al* 2008, and Jones M and Wilson M, 2005 and it was observed in a pilot study on our data) in two different conditions:1) we simulated Sirota's criteria by building a population of 10000 angles from which we extracted a single sample of arbitrary size (ranging from 200 to 3000) in which it was performed a bootstrap Rayleigh test by subsampling each sample 500 times with a subsample of size 100. Figure 3 shows an example of uniform and von Mises distribution of simulated data. We computed the median of pvals and observed that the test rejects the null hypothesis confidently (α=0.05) only for populations with $k >= 0.4$. For populations with $k<0.4$ power of the test is reduced regardless of the sample size (Fig 4a and b). 2). Given the results from

the simulation 1, we established which is the minimum sample size of a von Mises population of different degrees of concentration in which the test has enough power to detect it. By computing Rayleigh test on 500 samples of 100 to 1100 angles, we modeled the unknown real population and built a sample distribution of pvals. We observed that for *k*=0.1 the median pval of samples with less than 1000 angles was above 0.05 (Fig 5a). Moreover we tested pval distribution of 1000 sample size against 900 sample size and found that they are significantly different (Kolmogorov-Smirnov test, KS=0.088, p=0.0391), confirming that in case of having a population with *k*=0.1, sample size has to be above 1000 for Rayleigh test to have enough power (Fig 5b). Besides, for *k*=0.2, median pval of samples of 300 angles was below 0.05 and only concentrations *k*>=0.4 rejected the null hypothesis confidently with sample size of 100, confirming the results observed in simulation 1(Fig 6).

Taking these simulations into account, and considering that the sample size neurons/conditions varied from 100 to 10000, we decided to take the following criteria: neurons with less than 1000 spikes per condition were not included in the analysis unless they were significant for Rayleigh test even with a low sample size. We discard in this way neurons in which Rayleigh test is not powerful enough; those that showed a trend on directionality but also those who didn't. Nevertheless, given the effect of sample size on the parameters computed, comparison between conditions (e.g., Touch periods vs. ITIs) for phase modulation were done on samples of equal size. Finally, in order to alleviate for sample bias bootstrapped procedure was applied, i.e. 500 iterations of certain sub-sample size were done and the median of the different parameters (Z, *k*) was reported.

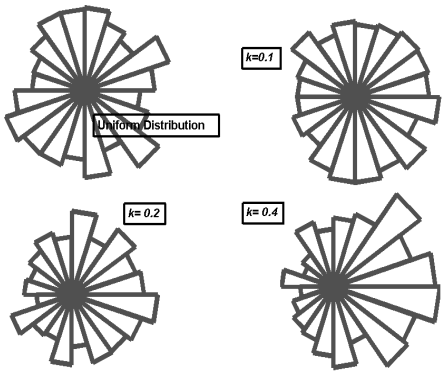

Figure 3: Uniform and von Mises distribution for kappa=0.1, 0.2 and 0.4. Simulated Data (n=1000)

a)

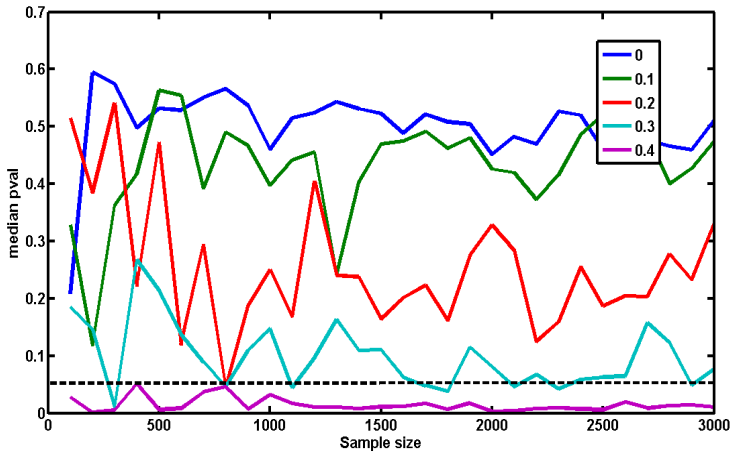

b)

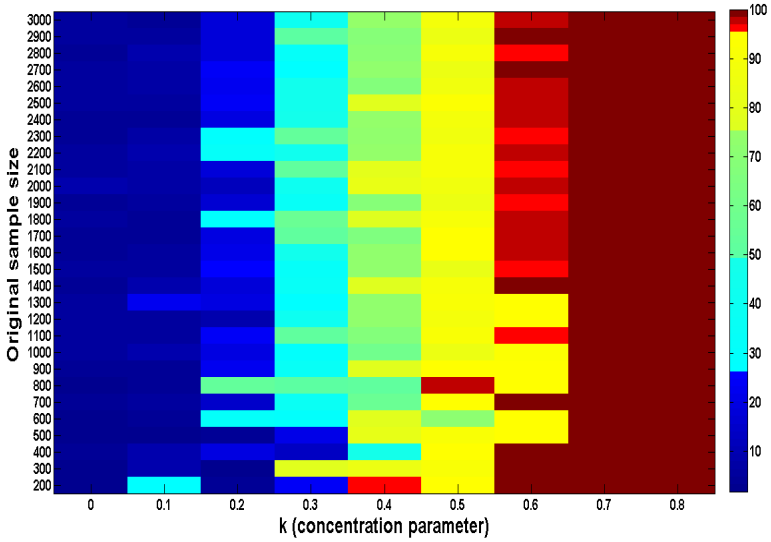

Figure 4: Simulation 1: We simulated a population of 10000 angles from which we extracted a single sample of arbitrary size (ranging from 200 to 3000) in which it was performed a bootstrap Rayleigh test by subsampling each sample 500 times with a subsample of size 100. a) Median of bootstrapped pvals. b) Percentage of pvals below α=0.05 obtained from bootstrapping each subpopulation. Rayleigh test rejects the null hypothesis confidently (α=0.05) only for subpopulations with k >0.4

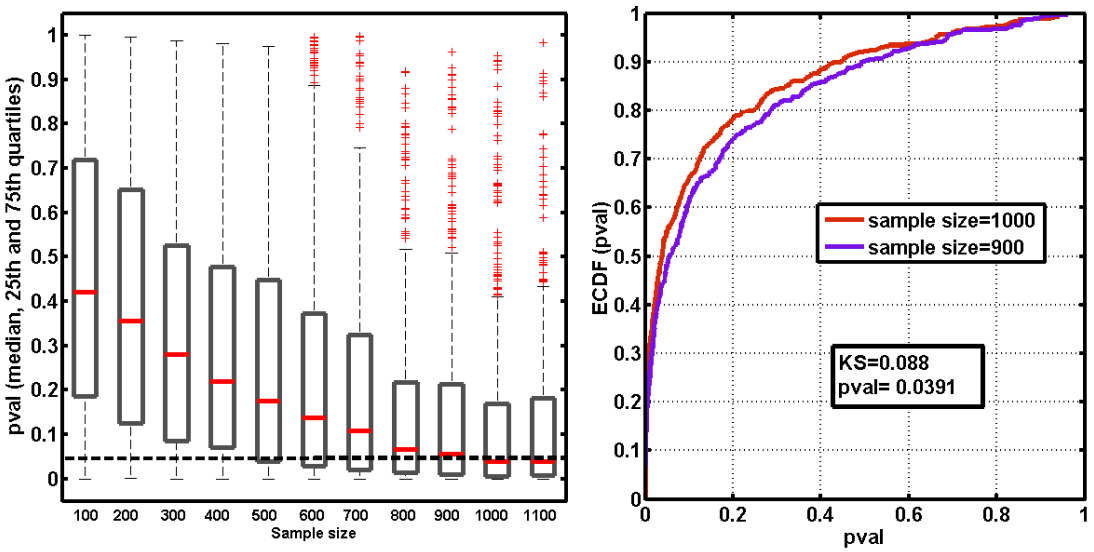

Figure 5: pvals from Rayleigh test computed on 500 samples of 100 to 1100 angles coming from a von Mises distribution of k=0.1. a) Median pval and 25th and 75th quartiles of pval distribution. b) Empirical cumulative distribution function (ECDF) of pval from 1000 sample size against 900 samples. Kolmogorov-Smirnov test, p<0.05.

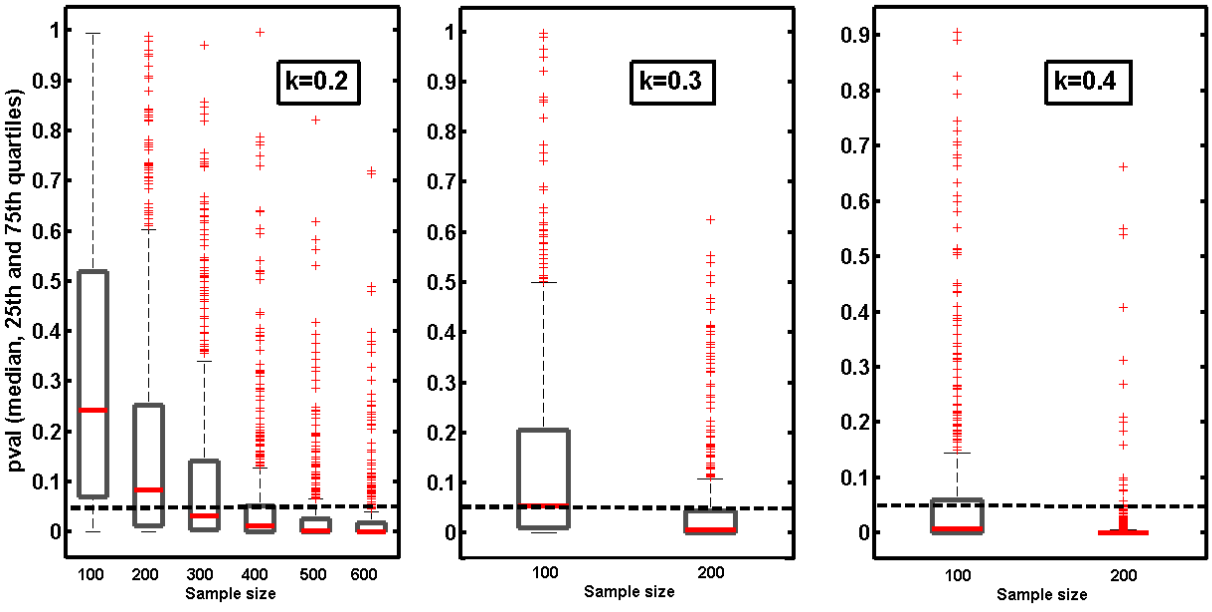

Figure 6: pvals from Rayleigh test computed on 500 samples of 100 to 1100 angles coming from a von Mises distribution with k= 0.2, 0.3 and 0.4.

Kuiper Test

Given an explanatory analysis of Rayleigh test, an important issue is that phase modulation of neurons may not follow von Mises distribution i.e. it could be bimodal or even multimodal. If we think about periodic fluctuations of sub-threshold voltages then we encounter certain time windows with equivalent state inside one period where neuron would fire. Also, one important consideration in this study is related to the fact that many of the units recorded are "multi-units". So there may be cases of 2 or more neurons fused with different preferred phases. Thus, the Rayleigh test for uniformity is the most powerful test only if the samples have a unimodal distribution. This will affect the measures derived from it like *k*. To alleviate some of these issues, we performed and additional test: nonparametric goodness-of-fit Kuiper's (Mardia KV and Jupp PE, 2000), which test for uniformity against any alternative. It tests the empirical cumulative density function (ecdf) of the sample against the cdf of the uniform distribution in the circular space. It is less biased to the sample size (Fig.7). The test statistic is:

$$V_n = D^+ + D^-$$

Where D+ and D- represent the absolute sizes of the most positive and most negative differences between the two cumulative distribution functions that are being compared. The statistic is the sum of both. If the value is low, then there is a good fit, whereas if the value is large, it may lead to significance. More correctly, the test statistic is

$$K = \sqrt[2]{n} * (D + +D-)$$

Kuiper is the circular version of Kolmogorov test.

Figure 7: From 'Directional Statistics', Mardia and Jupp, page 103.

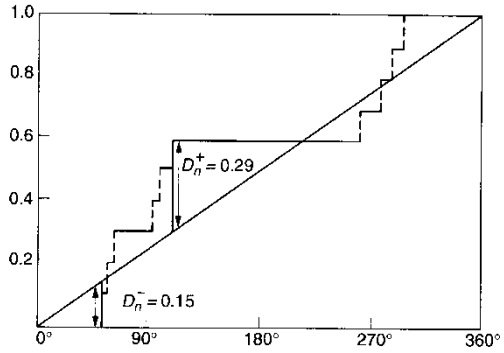

igure 6.2 Empirical and cumulative distribution functions for the pigeon-homing data of Example 6.1.

Correlation between Rayleigh and Kuiper

The percentage of neurons with significant theta-entrainment reported here comes from both tests described above: Rayleigh test and Kuiper test. While the first one test circular uniformity against the von Mises distribution, and therefore, assumes that the sample is generated from a unimodal distribution, the second one is a nonparametric goodness-of-fit test which test for uniformity against any alternative. Even if both test were strongly correlated ($r>0.9$, $pval<0.00001$), Kuiper test detected neurons which spikes distribution didn't fit the unimodal model. As Sirota et al (2008) pointed out: "because the firing of every neuron is driven presumably by a combination of phase-related and phase-independent inputs, a mixture model may be more accurate from the physiological point of view for the description of phase-modulation".

Author's comment: To better disentangle this issue, my proposal is: for those neurons that were significantly non-uniform distributed by Kuiper test but Rayleigh test failed to fit the von Mises model spike phases could be evaluated for modal groups (the first and simplest would be two modal groups) and grouped to then test separately for von Mises distribution. In this case, two concentration parameters and two mean directions would better describe the sample distribution.

Relationship between Theta Power and Spike Phase

Once neurons were analyzed for phase-locking, they were divided in "Theta-entrained neurons" and "Non-Theta entrained Neurons" groups to test separately for phase-power correlation. Spikes from Touch period were divided in two groups according to theta power (medium-low and medium-high). The power of each Touch period (1.2 sec) was extracted from the whole session power spectrogram: 5 slepian tapers were multiplied to a 1 sec - 3 Hz sliding (0.1sec) window before Fourier transform between 5 and 12Hz. Applying five independent tapers allowed us to reduce variance in the estimation of the power of each single period. Once the mean and standard deviation across all Touch periods were calculated, periods having theta power between the mean plus 2.5 std were grouped as 'high' and those with power between mean minus 2.5std were grouped as 'low'. So neuron spikes that fell into low group were grouped as 'low' and the same for spikes falling into Touch period with high power. The two groups were analyzed separately for non-uniformity, and finally, were evaluated with Wilcoxon signed rank test. Wilcoxon signed rank test is a two-sided signed rank test of the null hypothesis that data in the vector x-y come from a

continuous, symmetric distribution with zero median, against the alternative that the distribution does not have zero median.

Relationship between Spike density and Spike Phase

As for Phase-Power correlation analysis, once neurons were analyzed for phase-locking, they were divided in "Theta-entrained neurons" and "Non-Theta entrained Neurons" groups to test separately for phase-density correlation. Once median firing rate across all Touch periods was computed, they were divided into 'Low firing rate' and High firing rate' according to its firing rate with respect to the median. The two groups (Modulated and Non-Modulated Neurons) were analyzed separately for non-uniformity with Rayleigh and Kuiper tests, and finally, were evaluated with Wilcoxon Signed rank test for any difference in the resultant parameters.

RESULTS

Texture Discrimination Task, Hippocampal Theta rhythm and Cortical Spike Trains

Data presented corresponds to five rats; four were trained in a two texture discrimination task, and one in a three texture discrimination task. Rats' performance of each recording session was calculated by means of a randomization method (observed % correct versus shuffled data, $p < 0.05$). All session's performance was above chance (table 1). Performance upon encountering individual textures for each rat was tested statistically (Binomial test) and in all cases exceeded chance level with $p<0.01$ (fig 1).

Recording session	rat 1 % correct	rat 2 % correct	rat 3 % correct	rat 4 % correct	rat 5 % correct
1	76.5	95.8	74.5	78.7	92
2	81.6	97.4	72.7	86.8	90
3	83.4	98.8	-	91.7	83.3
4	86	100	-	80.2	89.7
5	81.5	93.5	-	80.7	90.8
6	-	97.4	-	-	93
7	-	87.9	-	-	94.7
8	-	92	-	-	88.4
9	-	89.8	-	-	96.2
10	-	85.3	-	-	-
11	-	88.9	-	-	-

Table1: Overall rat's performance in each session. The observed percentage of correct trials probability was calculated from the distribution of percentage of correct trials coming from a shuffled data. In all cases % of correct trials had $p<0.0001$.

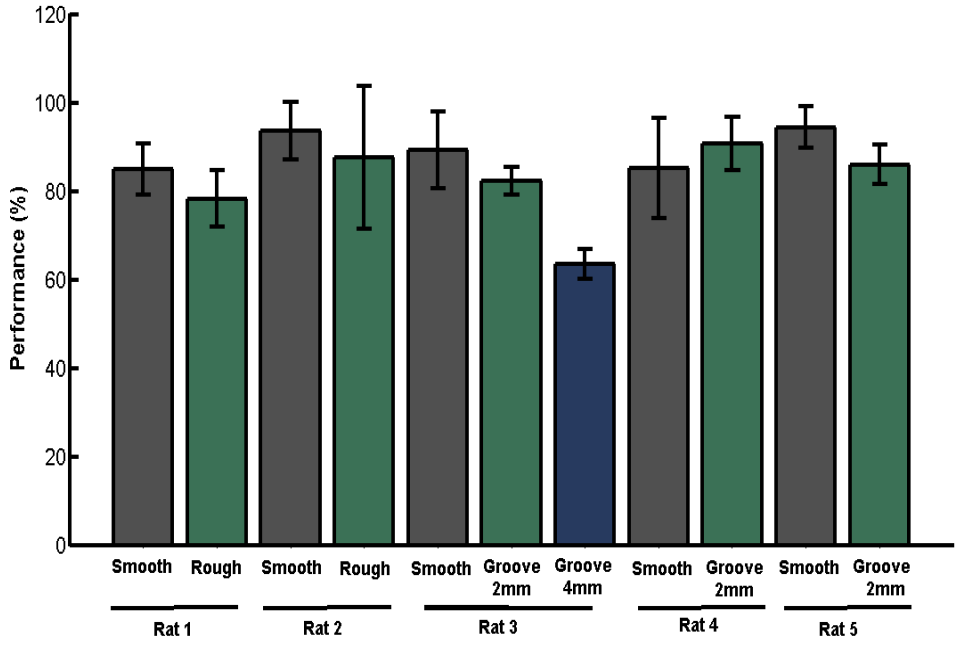

Figure1: Performance upon encountering individual textures for each rat. In all cases performance was above chance level (Binomial test, $p<0.01$).

We recorded simultaneously the activity of neurons from Primary somatosensory (barrel) cortex and local field potentials (LFPs) of dorsal hippocampus (CA1). S1 neurons were analyzed for its modulation by contact with textured plates and were classified as 'Contact responsive' or 'Contact Non-responsive', by comparing its firing rate during Touch period and a period before Trial started (Baseline period) with Paired t-test (Fig2 a and b). 132 out of 232 were contact-responsive, and 100 out of 232 were contact-non responsive during active touch of the discriminandum. To characterize the timing relationship, LFPs from Hippocampus was filtered between 5 -12 Hz (Fig2c) and theta signal was decomposed into instantaneous amplitude and phase components with Hilbert transformation. Spikes were assigned phase value $\Phi(t)$ (Fig2d) and the mean resultant vector was computed as the average of the vector sequence of spikes, and the mean preferred phase and length of mean resultant extracted. Phase locking to theta rhythm was analysed with Rayleigh and Kuiper Test.

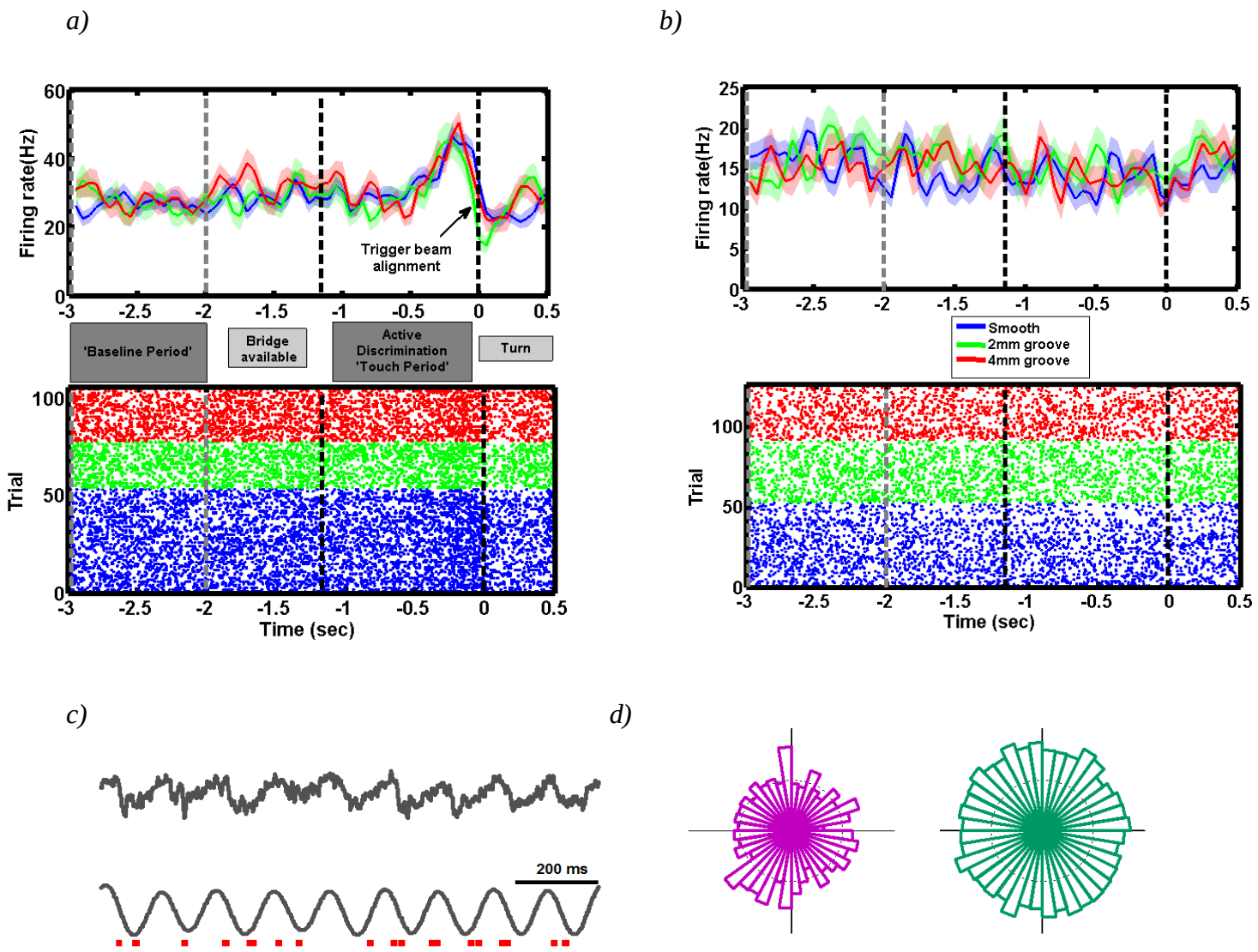

Figure 2: PSTH and raster plots of two S1 neurons while the rat is performing the three texture discrimination task. a) 'Responsive neuron': example of neuron with increased firing rate during touch (paired ttest $p<0.01$). b)'Non-Responsive neuron': example of neuron with no change in firing rate (paired ttest $p>0.01$) during touch. c) simultaneous recording of CA1 LFP (raw and theta filtered LFP trace) and spiking activity of an example neuron during the tactile discrimination task. d) Example of spike-phase distribution during Touch period (left) and ITI (right).

Phase-Locking of Primary Somatosensory Cortex neurons to Hippocampal Theta during Active Texture Discrimination

After an exploratory analysis of spike phases distribution, 232 neurons from primary somatosensory cortex were analysed for phase locking to hippocampal theta in the period from which the animal was about to touch the texture, and then actively sensing the discriminandum till decision making (1.2sec total duration), i.e. till withdrawal to collect water.

Of 232 neurons, 41 S1 neurons (18%) were significantly locked to hippocampal theta during Touch period (Rayleigh/Kuiper test, $p<0.05$). 25 out of 41 were 'contact responsive', while 16 out 41 were 'contact non responsive', meaning that 19% of contact-responsive neurons and 16% of contact non-responsive were significantly theta-entrained. Both groups had equal concentration parameter and Kuiper statistic distribution (Fig 3a: Kolmogorov-Smirnov test, KS= 0.1859, p=0.8367, fig 3b: KS=0.1741, p= 0.8886) and equal firing rate distribution (Fig 3c: Kolmogorov-Smirnov test, KS=0.1775, p= 0.8872), indicating that the degree of phase locking was not associated to transient increase in spike density.

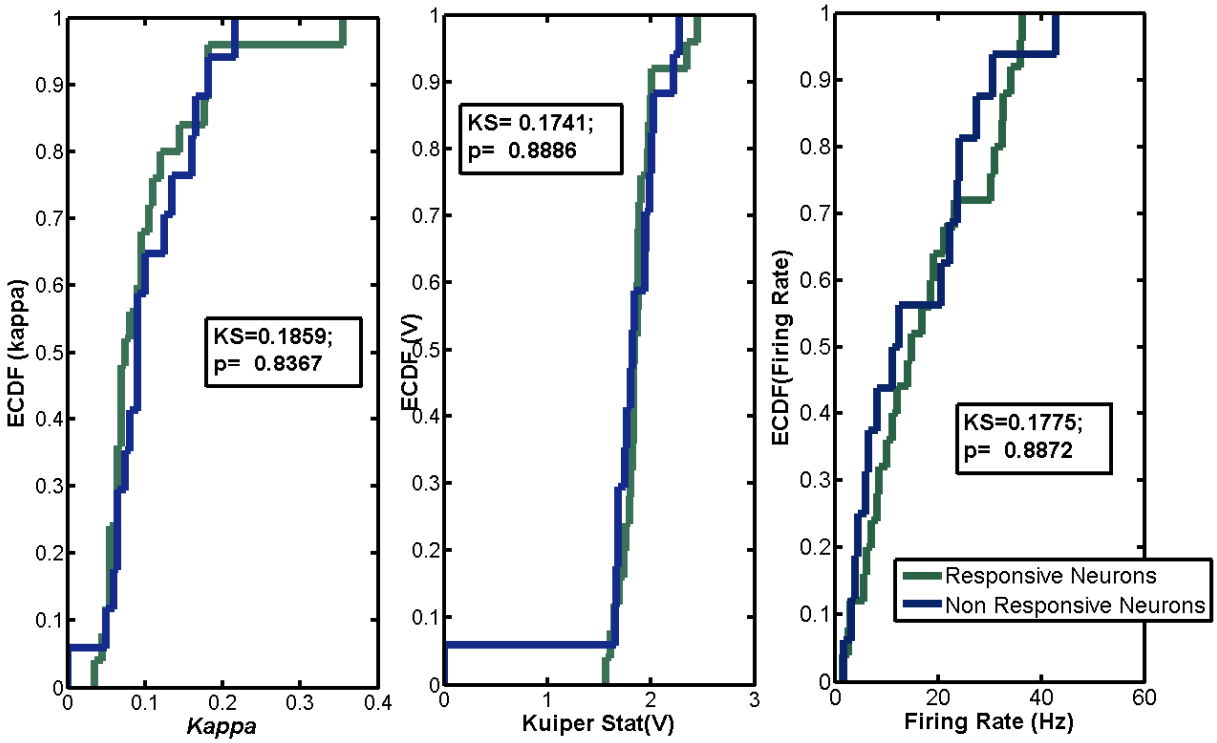

Figure 3: Empirical Cumulative Distribution functions of a) Kappa, b) V statistic and c) mean Firing Rate, for Neurons that were significantly locked to hippocampal theta. ECDF comparison of 'Responsive' and 'Non Responsive' neurons were analyzed with Kolmogorov-Smirnov test ($p<0.05$).

Now, if we think about the periodicity of 4 to 12Hz theta rhythm as a reference signal, then a group of S1 neurons locked in a certain range on the theta cycle would have mutually increased firing probabilities every a certain window length. The net effect would be an increased correlated activity inside the region and a potential increase in the efficiency of information transfer. Although we observed that S1 neurons tended to fire in the same range of theta cycle; to the upward (>270º) phase of theta (Fig 4), Rayleigh and Kuiper tests failed to detect a non-uniform distribution. However, this approach ignores the information from the strength of theta entrainment of each individual neuron. We applied a modification of the Rayleigh test (Batschelet E, Circular Statistics in Biology, page 212): each single neuron preferred angle was multiplied by a rank value corresponding to the Z_{ith} value. Z_i values were ranked from smallest to largest. We tested in this way whether preferred angles are independently and uniformly distributed on the circle, and further, that preferred angles do not depend on the strength of theta phase locking. Still we could not reject the null hypothesis in favor of a population preferred theta angle of firing.

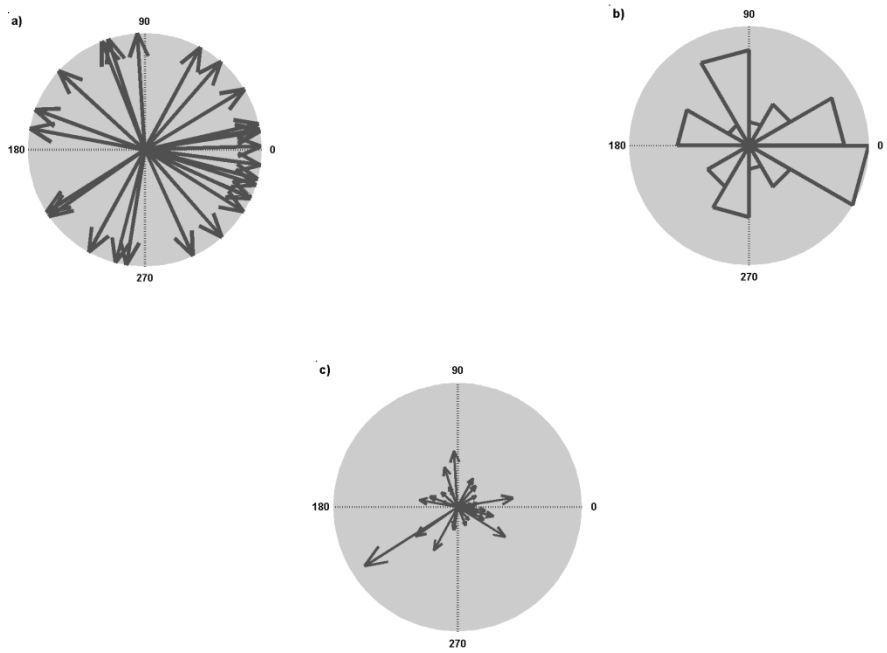

Figure 4: Preferred mean angle distribution of theta-entrained neurons (n=28). a) All neurons preferred angle represented by unit length vector. b) Binned preferred angle distribution of theta-entrained neurons. c) All neurons preferred angle weighted by the strength of theta-entrainment.

We further addressed this issue, this time asking whether there are different functional phases for somatosensory neurons that show stimulus related increase in firing rate with respect to neurons that do not increase significantly its firing rate. Interestingly, 'contact responsive' and

'contact non- responsive' groups showed a clear opposite phase range of the theta cycle; contact responsive neurons tended to fire in the upward phases of the cycle whereas contact non-responsive neurons tended to fire in the downward phase of the cycle (Fig 5).

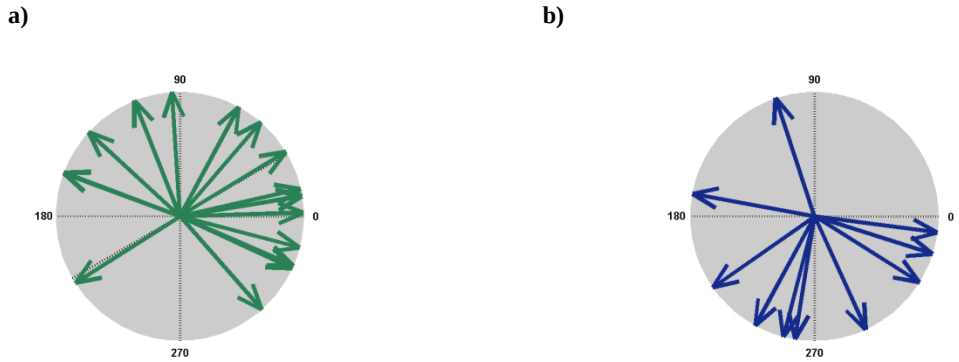

Figure 5: Preferred mean angle distribution of contact responsive and contact non-responsive neurons (n=28). All neurons are theta-entrained neurons and its preferred angle is represented by a unit length vector. a) Contact responsive neurons. b) Contact non-responsive neurons.

Phase-Locking of Primary Somatosensory Cortex neurons to Hippocampal Theta during Quiet Wakefulness

Periods of 'rest' in the middle of the recording session of the tactile discrimination task were taken for the analysis of theta- entrainment as opposed to Touch periods in which sensory and cognitive processes are taking part. We observed that in these periods of quiet wakefulness (ITIs) 12 S1 neurons out of 118 (10.17%, 58.33% 'contact responsive' and 41.67% 'contact non responsive') were significantly locked to hippocampal theta. 33.33% (4 out of 12) of these neurons corresponded to neurons significantly locked during 'Touch' period. If the consistent timing relationship between neural spiking and ongoing theta rhythms provides a mechanism through which to coordinate S1 and CA1 activity, and if the coordination between these structures depends upon task demands, the degree of phase-locking might be expected to be stronger during Touch period. As expected, neurons that were significantly locked during 'Touch' period, showed significantly stronger theta-entrainment in the touch with respect to the ITI period when equal sample size for both conditions were taken and analysed (Fig 6, Wilcoxon signed rank test $p<0.05$).

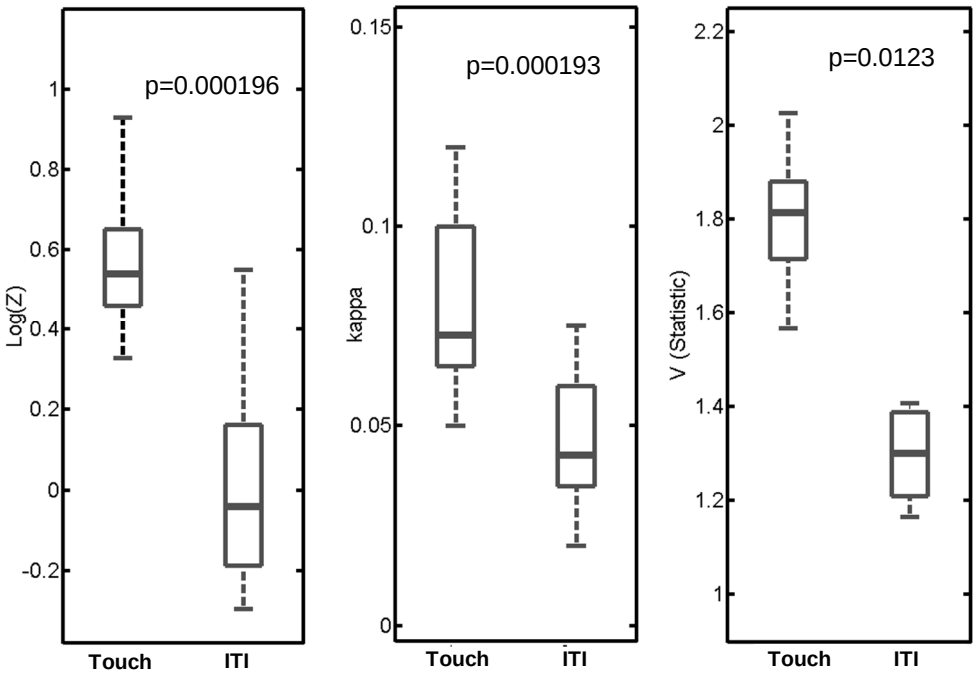

Figure 6: Spike-theta entrainment comparison between Touch and ITI for neurons that were significantly phase-locked during Touch period but were not significantly phase-locked during ITI. Graph shows median and quartiles of Rayleigh statistic Z, k and Kuiper statistic (V). Paired comparison of both conditions was computed for which each neuron had equal sample size. Only neurons that were significantly locked to theta during Touch (LogZ, k: n=29, V: n=41, Wilcoxon sign rank test $p<0.05$) are shown here.

Figure 7 shows three neurons significantly locked during Touch period in contrast with ITI periods. Moreover, we compared the degree of phase locking for those neurons that were significantly locked to theta during ITI with respect to Touch period. As seen in Fig 8, there was no significant difference for any of the parameters during ITI compared to Touch period. Furthermore, we found that the neuronal population modulated during Touch period was more strongly theta-entrained than the neuronal population that was modulated during ITI (Fig 9). This result further supports our hypothesis of spiking activity modulation during periods where coordination between areas might be critical. Not only a higher number of neurons are modulated during touch compared to ITIs but also they are more strongly modulated.

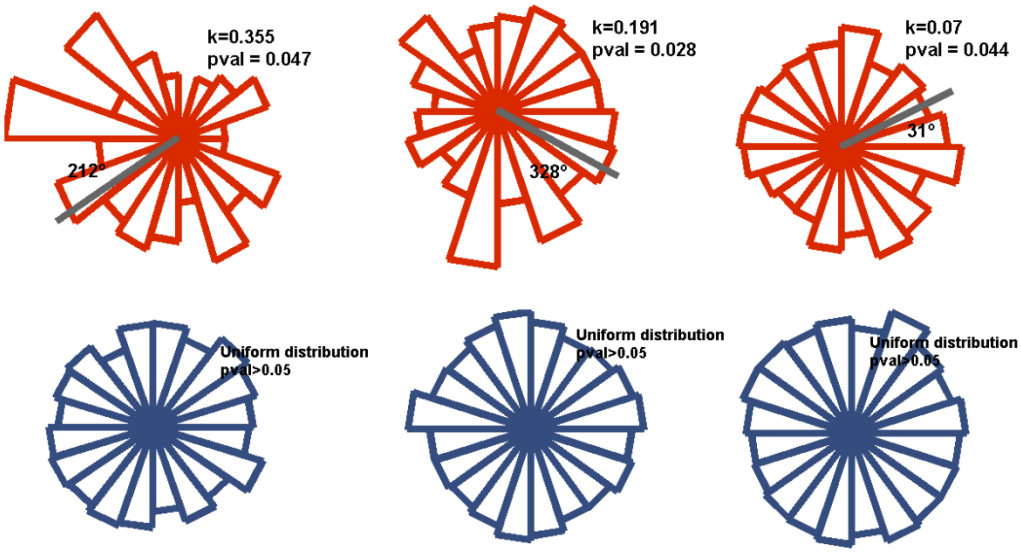

Figure 7: Three neurons significantly theta-entrained during Touch period in contrast to ITI were uniformly distributed (Rayleigh/Kuiper test, p>0.05)

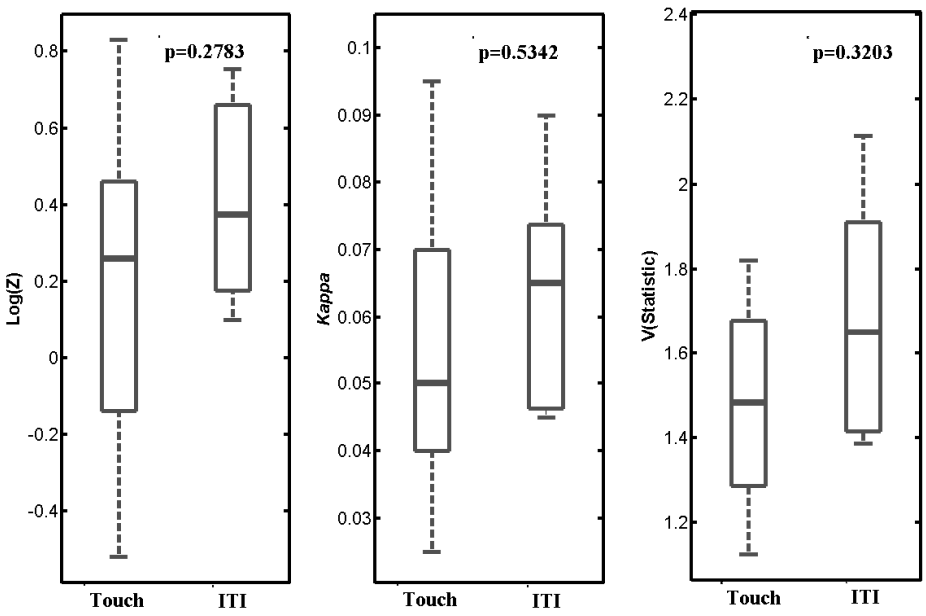

Figure 8: Spike-theta entrainment comparison between Touch and ITI for neurons that were significantly phase-locked during ITIs. Graph shows median and quartiles of Rayleigh statistic Z, k and Kuiper statistic (V). Paired comparison of both conditions was computed for which each neuron had equal sample size. Only neurons that were significantly locked to theta during ITI (n=11, Wilcoxon sign rank test p<0.05) are shown here.

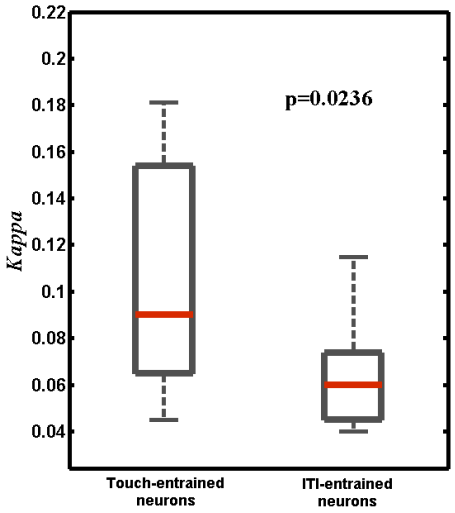

Figure 9: Strength of spike-theta entrainment (k) comparison between neuronal population theta-modulated during Touch and ITI, k and Kuiper statistic (Touch: n=28, ITI: n=11, Wilcoxon sign rank test p<0.05) are shown here.

Relationship between Spike density and Spike Phase

We studied the effect of spike firing fluctuations on the degree of phase locking during Touch period for significantly theta entrained neurons. Each single Touch period FR was classified as Low or High by comparison with the average firing rate. Spikes that fell into periods with FR less than mean FR were grouped together as 'low FR' group. On the other hand, spikes belonging Touch periods with FR major to the mean FR were grouped as 'high FR'. By analyzing Rayleigh and Kuiper parameters with equal sample size we observed that higher FR or higher spike density didn't result in higher degree of theta-entrainment (Fig 10)

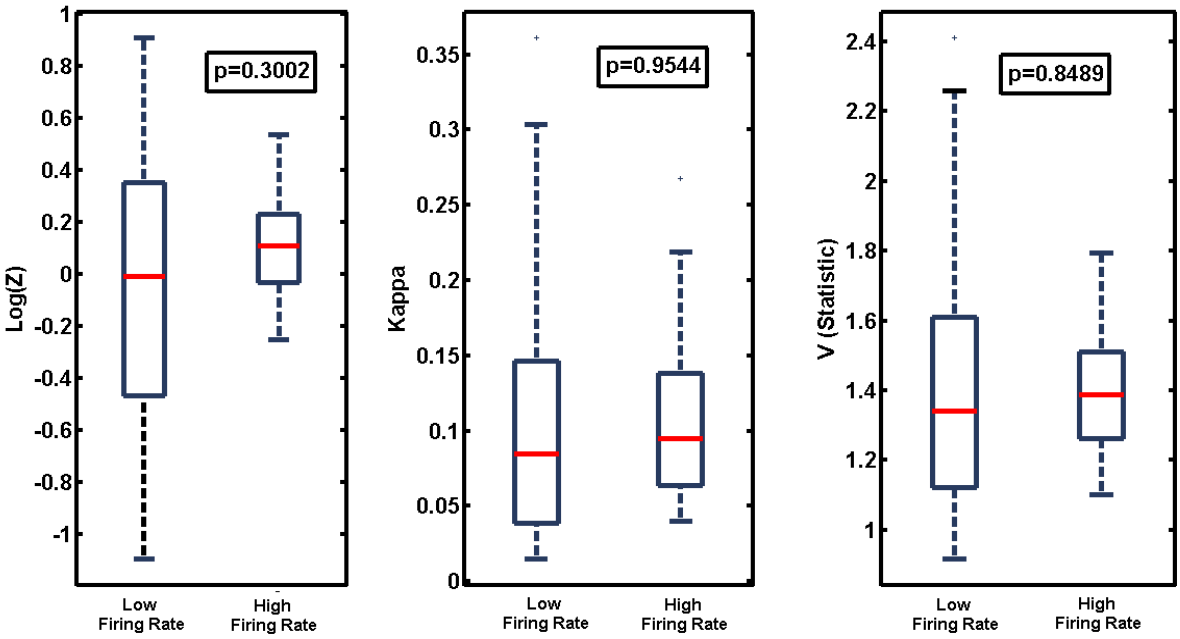

Figure 10: Spike-Phase Firing Rate Correlation. Graph shows median and quartiles of resultant Rayleigh statistic (LogZ), the concentration parameter (k), and Kuiper statistic (V) in both conditions: Low and High firing rate (Wilcoxon Sign rank test. Z and k: n=25. V:n=26)

Spike Phase- Power Correlation during Touch Period

Higher theta power and consequently a stronger rhythmic input could be the way by which hippocampus modulates more efficiently neurons from other regions. To test this hypothesis we measured the degree of spike-phase locking of each single neuron (those that were in previous analysis to be significantly locked to theta) in case of trials with high theta power and low theta power. In other words, we measured the relationship between strength of theta-entrainment and theta power. Spikes from Touch period were divided in two groups according to theta power and classified as 'high' or 'low'. The two groups were analyzed separately for non-uniformity, and finally, were evaluated phase-power correlation with Wilcoxon rank test for equal medians. As shown in Fig 11, degree of theta entrainment didn't change with an increase in theta power for the neurons that were significantly entrained to theta rhythm. Discarding the possibility that improved reliability of phase measurements resulting from an increase in hippocampal theta power increases the degree of theta entrainment.

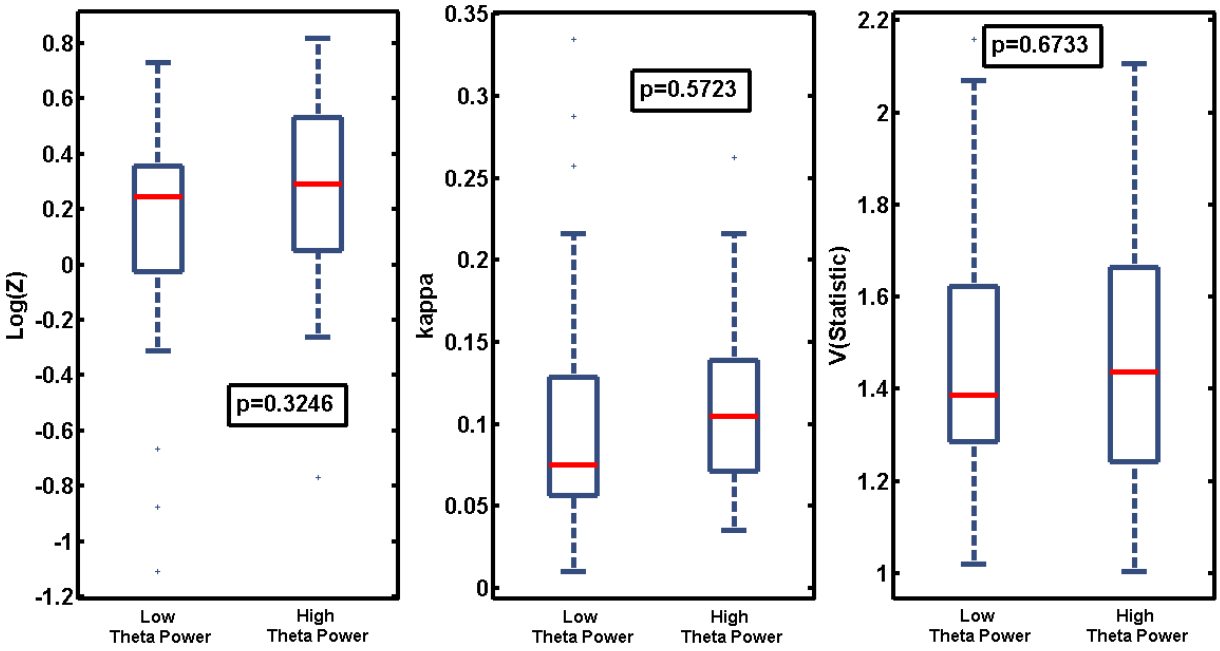

Figure 11: Spike-Phase Power Correlation. Graph shows median and quartiles of resultant Rayleigh statistic (LogZ), the concentration parameter (k), and Kuiper statistic (V) in Low/High power conditions for Theta-entrained neurons. (Wilcoxon Sign rank test. Log(Z) and k: n=27. V:n=30)

Theta Power during Intertrial period

In an attempt to further characterize theta rhythm from CA1, we computed the average spectrum of ITIs periods cut into 1.2 second applying 2 tapers (slepian tapers) to a 1.2sec-3Hz window before the Fourier transform. We did the same analysis for Touch period (1.2 sec-3Hz window) and tested for significant difference performing a Montecarlo test with Bonferroni correction for multiple comparisons (Fieldtrip Toolbox). Figure 12 shows, the average spectrum of ITIs and Touch period. As expected, hippocampal theta power decreases significantly during ITIs where rats are in a state of quiet wakefulness.

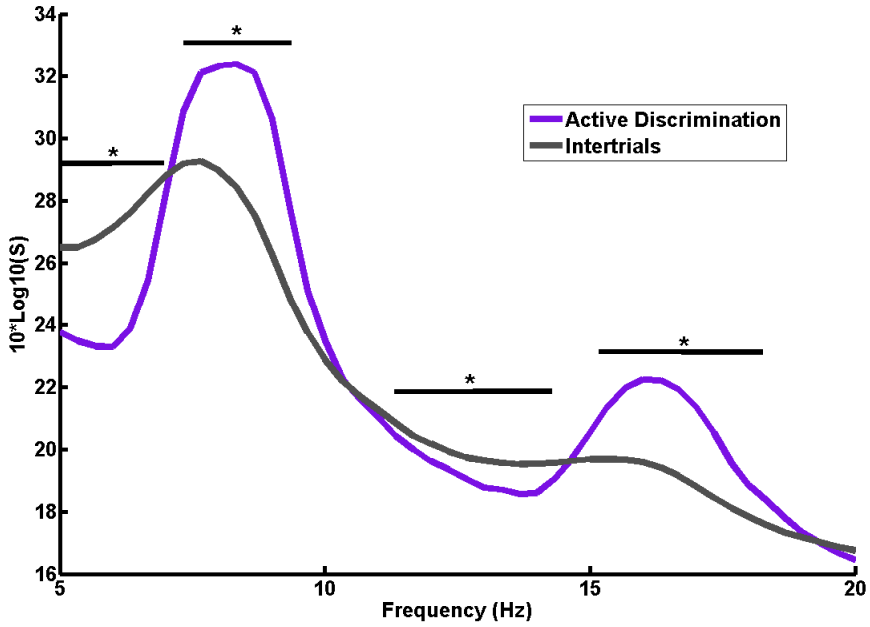

Figure 12: Average spectrum of ITIs compared to Touch periods (Active discrimination). LFP signal was cut into 1.2 second applying 2 tapers (slepian tapers) to a 1.2sec-3Hz window before the Fourier transform. Touch period (1.2 sec-3Hz window) and tested for significant difference performing a Montecarlo test with Bonferroni correction for multiple comparison (Fieldtrip Toolbox).

CONCLUSION AND DISCUSSION

Setting simultaneous recording of cells from barrel cortex and hippocampus during a tactile discrimination task allowed us to investigate how oscillations from Hippocampus influence vibrotactile processing in the context of a discrimination task.

Here we provide evidence that the firing of a significant fraction of S1 neurons is dynamically modulated by hippocampal theta rhythm according to the behavioural demands. 18% of barrel cells were significantly locked to hippocampal theta during active discrimination period. This percentage is in accordance with Sirota et al (Sirota A, Montgomery SM, Fujisawa S, Isomura Y, Zugaro M and Buzsáki G, 2008), in which they reported that the percentage of significantly modulated cells was 32% for interneurons and 11% for pyramidal (data coming from different sub-regions of parietal cortex). Interestingly, we observed that 19% of 'contact responsive', and 16% of 'contact non responsive' were phase-locked to theta rhythm with no significant differences in the degree of phase-locking and equal firing rate distribution. This result suggests that selective entrainment of the subset is not associated to stimulus related transient increase in firing rate. Moreover when touch periods were divided according to its FR as with 'low' or 'high' FR, degree of phase locking didn't change significantly. This type of analysis allowed us to disentangle a potential effect of spike density on the degree of theta-entrainment in contrast to the commonly used measure "spike-field coherence". Spike-field coherence, which is a frequency domain measure of consistent neural spiking at a specific phase of the LFP (Jarvis M and Mitra P, 2001) (Fries P, Womelsdorf T, Oostenveld R and Desimone R, 2008) has been extensively used to understand neuronal group interactions but it has been argued that is dependent on neuron firing rate (Lepage KQ, Kramer MA, Eden UT, 2011).

CA1-S1 synchrony during specific behavioural epochs

Importantly, we found that during periods of rest interleaved in the second half of the discrimination task, neurons decreased significantly the degree of phase-locking with respect to active discrimination period. This result supports the hypothesis that different structures may increase the efficiency of information transfer by way of rhythmic mechanisms that dynamically entrain them. How synchrony is enhanced during active sensation? One possibility is simply by enhancing theta power during active sensation. However, in testing this hypothesis we encounter a potential confound and this comes from the possibility that improved reliability of phase measurement resulting from an increase in theta power increases the degree of theta entrainment. On one hand we found that theta power during ITI period was significantly lower than during

Touch period. On the other hand, we found that touch periods were insensitive to theta power changes. This result suggest that 1) phase-synchronization during touch period is not dependent on fluctuations of theta power, and that 2) power changes during touch periods do not affect theta phase-locking measures. However this second point may not extend to ITIs if both high and low theta power trials have larger theta amplitudes than the ITIs. A better control for this issue would be to take only ITIs of comparable theta power as the considered Touch period. As for the first point, many works have shown that phase-locking of neurons to the oscillatory rhythm was not dependent on power (Hyman JM, Zilli EA, Paley AM, and Hasselmo ME, 2005) (Jones M and Wilson M, 2005).

Differential phase- locking dependent on contact responsiveness

'Contact responsive' and 'contact non- responsive' groups showed a clear opposite range of phases of the theta cycle during touch period; contact responsive neurons tended to fire in the upward phases of the unit cycle whereas contact non-responsive neurons tended to fire in the downward phase of the unit cycle.

If we think about the periodicity of 4 to 12Hz theta rhythm as a reference signal, then a group of S1 neurons locked to a range of theta phases will have mutually increased firing probabilities every a certain window length. The net effect will be an increased correlated activity inside the region and a potential increase in the efficiency of information transfer, reciprocal (Fries P, 2005), (Isomura Y, Sirota A, Ozen S, Montgomery S, Mizuseki K, Henze DA and Buzsaki G, 2006), (Sirota A, Csicsvari J, Buhl D and Buzsaki G, 2003), (Sirota A and Buzsaki G, 2007), (Womelsdorf T, Schoffelen JM, Oostenveld R, Singer W, Desimone R, Engel AK and Fries P, 2007) or unidirectional, between primary somatosensory cortex and upstream regions. Theta rhythm segregates in a specific time window somatosensory neurons carrying texture information (von Heimendahl M, Itskov PM, Arabzadeh E, Diamond ME, 2007) (Diamond ME, von Heimendahl M, Magne Knutsen P, Kleinfeld D and Ahissar E, 2008).These results suggest that there is a interplay between hippocampal theta coupling and the input coming from the tactile stimulus at the cellular level. Studies on the molecular mechanism by which neurons that receive sensory input are 'clustered' in a certain time window would be highlighting in the context of how the brain constructs a representation of meaningful stimuli.

Which are the mechanisms responsible for S1 phase locking?

Multiple mechanisms could be responsible for S1 theta entrainment. A potential mechanism for such distant neurons may entail entorhinal cortex (EC) and/or PFC by way of their widespread and mostly reciprocal connections with primary (and secondary) sensory areas (Groenewegen HJ

and Uylings HB, 2000), (Swanson LW and Kohler C, 1986), (Witter MP, 1993). Also sparse long-range hippocampal projections to distant neocortical regions could be responsible for imposing the hippocampal rhythmic output (Cenquizca LA and Swanson LW, 2007), (Jinno S, Klausberger T, Marton LF, Dalezios Y, Roberts JD, Fuentealba P, Bushong EA, Henze D, Buzsaki G and Somogyi P, 2007).

The selectivity in theta-entrainment could be due either to stronger synaptic connectivity between hippocampus and the selected target or by intrinsic properties of neural subgroups (Ulrich D, 2002). In particular, it has been shown that pyramidal neurons in layer 5 somatosensory cortex display sustained, prolonged, 5- to 12Hz patterns of either single spikes or bursts of spikes in vitro. These intrinsically rhythmic neurons can generate cortical oscillations and project them to neurons of other layers. Synchronized rhythmicity is dependent on tonic activation of NMDA receptors by endogenous glutamate, and this could provide a mechanism of selective modulation by hippocampus.

Chapter IV

Relationship between Whisking and Hippocampal Theta Rhythm

MATERIALS AND METHODS

See Chapter II (General Methodology) for Training procedure, Surgery and Recording.
All analysis was performed using custom-written tools in Matlab (Mathworks) unless stated.

Experiment

Discrimination Task

3 rats were trained to perform a tactile discrimination task 1) rat 4 and 5 were trained in a two textures scheme (smooth surface to right reward and 4mm groove surface to left), 2) rat 3 was trained in a three texture scheme associated with two opposite reward places (2mm grooves and smooth surface-to right reward and whereas 4mm groove surface to left).

Free moving Arena:

The two rats (rat 4 and 5) trained in the two texture tactile discrimination task were also trained to whisk on the air while walking back and forward on a squared platform (Figure 3). (40cmx40cm) in which cereals scales were delivered randomly (see picture) Hi-speed camera (200fps- 512X512 pixels, Motionpro 2000; Redlake) was positioned on top in order to capture whiskers motion.

Whisker Tracking

In order to extract whisker movement from both tasks two different approaches were taken due to technical constrains. We performed automatic tracking in the case of Discrimination task whereas for the free moving Arena we performed whisker movement extraction manually.

Videography and Automatic whisker tracking:

For the extraction of whisker movement during discrimination task we recorded films for each trial with a hispeed camera (Optronis CamRecord 450, Optronis) with resolution set to 510 × 256. The spatial resolution varied between 0.12 and 0.25 mm/pixel and sampling frequency equal to 1,000 fps. Camera was positioned in order to take a top view of the discriminandum and its surroundings. Films were recorded with infrared light reflected in a circular mirror positioned under the rat; the head of the rodent and its whiskers are dark against a bright background. In all trials, the rat entered the field of view from the upper edge, approached the texture, and withdrew after making a few contacts, turning right or left for a water reward. Film length had a total of 750msec,

but only 680msec (rat 4) and 562msec (rat 5) confined to contact period were taken for the analysis. Central sensor was used to synchronize behavior, electrophysiological recordings and hi-speed films. We extracted automatically whisker movements using the algorithms created by Perkon et al (Perkon I, Kosir A, Itskov PM, Tasic J and Diamond ME, 2011) in our laboratory and inserted in the Standard Tracker free toolbox. The software was written using MATLAB (MathWorks, Natick, MA), with extensive use of the Image Processing Toolbox and the Spline Toolbox. The program provides full quantification of head orientation and translation, as well as the angle, frequency, amplitude, and bilateral symmetry of whisking. As for testing our hypothesis we extracted the mean angle of whisker movement.

Videography and Manual whisker tracking

For the extraction of whisker movement during 'Free moving Arena' we recorded films for each trial with a hispeed camera (Optronis CamRecord 450, Optronis) with resolution set to 800 × 600. The spatial resolution varied between 0.12 and 0.25 mm/pixel and sampling frequency equal to 200 fps. Camera was positioned in order to take a top view of the discriminandum and its surroundings. Platform had a red glass floor and was illuminated from above in order to get the rodent and its whiskers dark against a bright background (Fig 1). As mentioned above rats were able to freely move around the platform for an average of 30 min each session (rat4: 5 session, rat5: 8 sessions). Each session collected a total of 150 seconds of hispeed film from which only periods of data were whiskers were visible were taken. Whisking pieces were grouped according to two overt behaviors: 'Walk' and 'Foot Planted' periods. In both cases whisking pieces were cut into 680msec (rat 4) and 562msec (rat 5) pieces termed 'trials' in order to make the spectral analysis comparable.

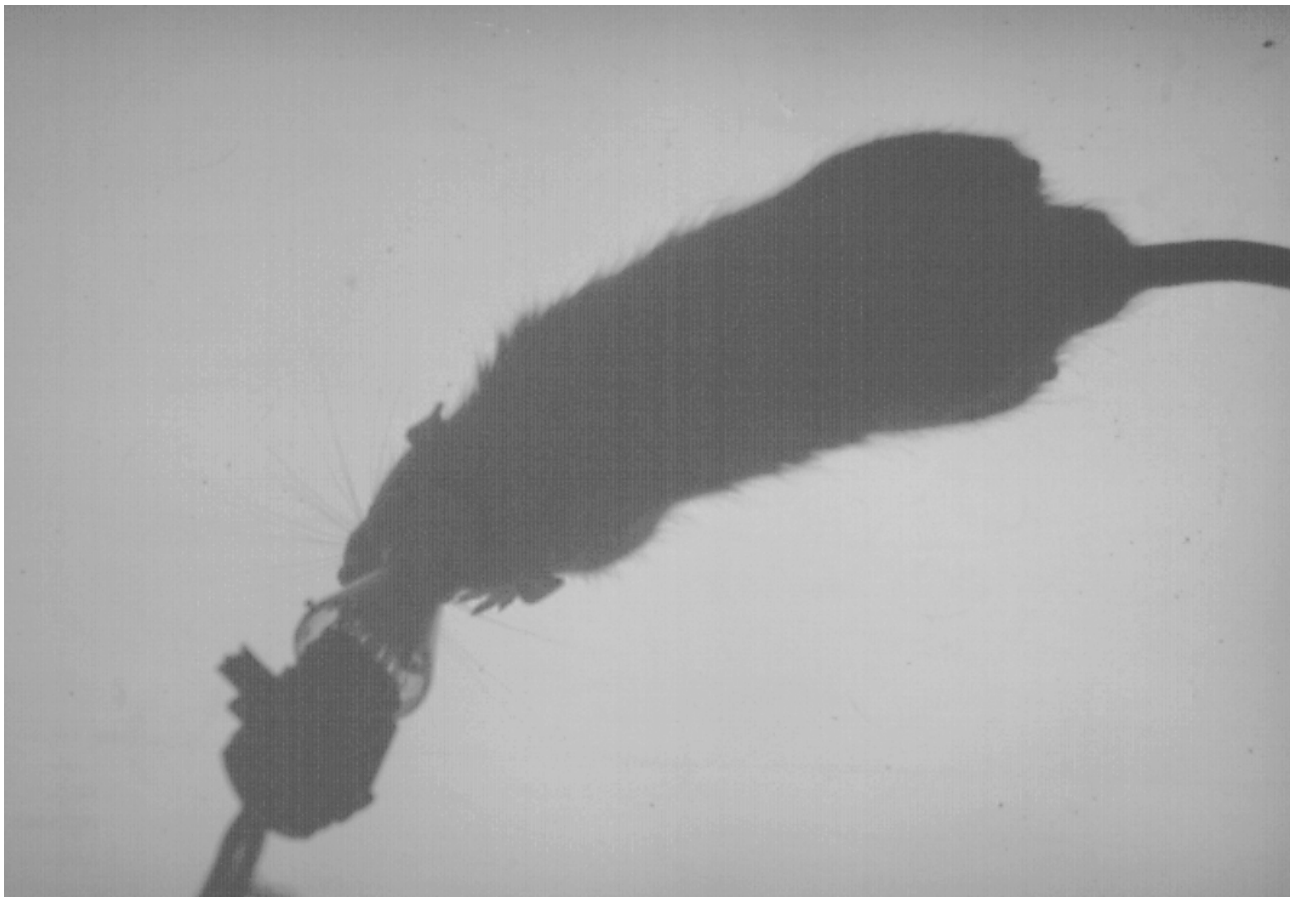

Figure 1: Snapshot of the Free moving Arena

Extraction of whisker movement consisted on the detection of retraction/ protraction start and end frame, and the reconstruction of the movement by modeling a sinusoid whisking movement. Only epochs with clear whisking activity without bumps in the trajectory were included.
Retraction,

***cos (pi*/(Retraction end Frame - Retraction start Frame)/fps+*pi*)**

Protraction,

***cos (pi*/(Retraction end Frame - Retraction start Frame)/fps)**

Figure 2 shows an example of whisking reconstruction,

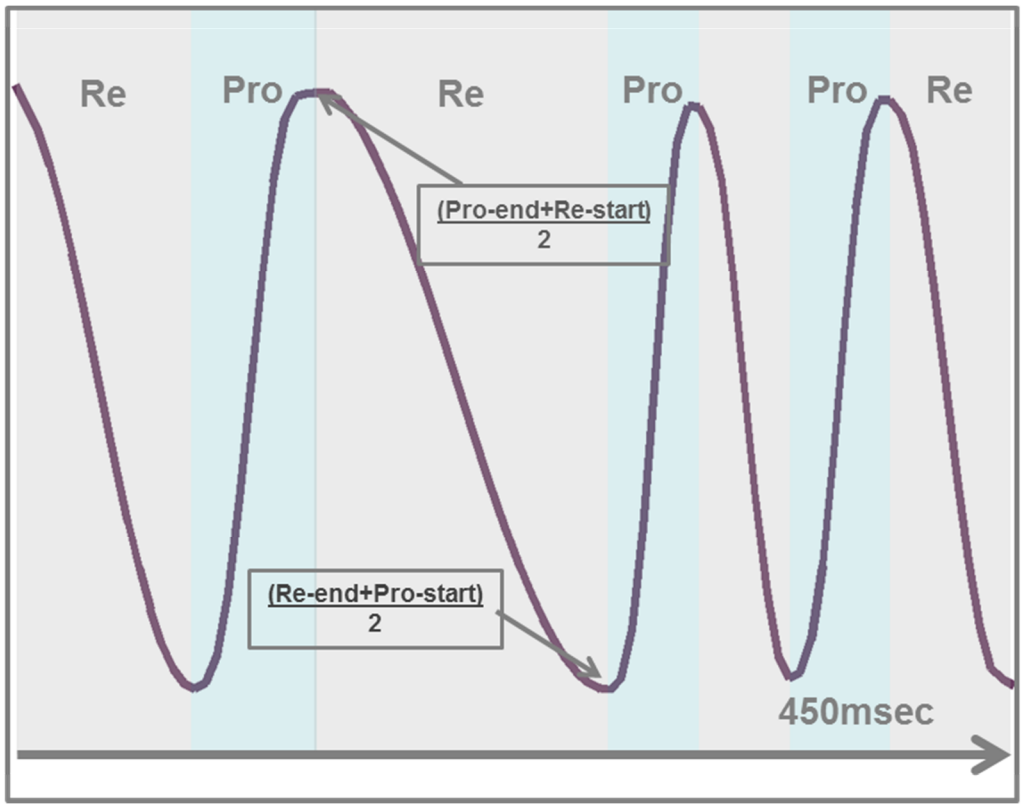

Figure 2: Example of whisking movement reconstruction. Re=Retraction, Pro=Protraction.

LFP Power Spectrum and Phase Locking value

For power spectrum we used 1 taper (Hanning taper) applied to a 0.56 or 0.68 sec time length and frequency resolution 2Hz and range 4-20Hz before the Fourier transform. We already explained the principles of Fourier Transform and power spectrum in General Methodology (Chapter I). We will now explain the principles of the phase locking value.

The Phase locking value (PLV)

To measure the relation between hippocampal LFP and whisking, we performed bivariate spectral analysis (Fieldtrip Toolbox). The basic idea in bivariate (and more general; multivariate) spectral analysis is that for multiple time series *xi*(*t)* once we have moved to the frequency domain, *Xi(f)* are uncorrelated for different frequencies for stationary processes. Thus, after Fourier transformation, we performed ordinary multivariate analysis: the covariance function between the two processes is known as the cross-spectrum. The cross-spectrum (of two signals *i* and *j*) is the Fourier Transform of the time domain cross-correlation function:

$$Xij(f)=E[Xi(f)*Xj(f')],$$

By taking,

arg(*Xij(f)*)

we ignore the magnitude of the spectrum (cross-spectrum in this case) in the computation of phase consistency. We measure phase consistency by means of the Phase Locking Value (PLV).

PLV(*f*)= |1/*N* *ΣXij(f)*|, were N=trials

The resultant vector length is a real number in the range of 0 (low phase consistency) to 1 (high phase consistency).

Amplitude Correlation

We computed power spectrum of both signals for each trial and extracted the power of peak frequency. Then we computed Spearman Correlation test for each animal.

Statistical Measures

Significance level of the PLV

By means of a Montecarlo test, we computed the significance level of Phase synchronization. The procedure consisted on shuffling LFP signal across trials 1000 times and computing the plv for each of the fake pairs of signals (LFP-whisking). By computing the probability of getting a value as extreme as the sample one on the population drawn from the shuffled data, we got the pval of the sample. We applied Bonferroni for multiple comparison correction.

Test for significant differences in the Power Spectrum and PLV between conditions

We tested for significant differences between any conditions performing a Montecarlo test (Fieldtrip Toolbox). In this case the significance probabilities and/or critical values were calculated by building random partitions: we randomly drew as many trials from the combined data set as there were trials in condition 1 and place them into subset 1and the remaining trials are placed in subset 2. We calculated the t statistic (two sample t-test) for the random partition and repeated the procedure 1000 times building a histogram of the test statistic. From the test statistic that was actually observed and the histogram, we calculated the proportion of random partitions that had a larger test statistic than the observed one. This proportion is the Monte Carlo significance probability, which is also called a *p-value*. We applied Bonferroni for multiple comparison correction.

RESULTS

Hippocampal Power Spectrum during the Tactile Discrimination Task and Free moving Arena

We first characterized the LFP signal from hippocampus in the different behavioral conditions. In the case of the tactile discrimination task we computed the LFP Power spectrum of the last 600msec before decision making reflects what is observed in the time frequency resolution: a theta range between 7-12Hz with a peak frequency at around 8 Hz (Fig 1b). We characterized also whisking activity by recording films for each trial with a hi-speed hi-resolution camera (Optronis CamRecord 450, Optronis) and from which we extracted whisker movement during last approach and contact time (600 msec before decision making) with the Standard Tracker toolbox. Power spectrum of rhythmic whisking during contact epoch was within the range of 7-12Hz (Fig 2).

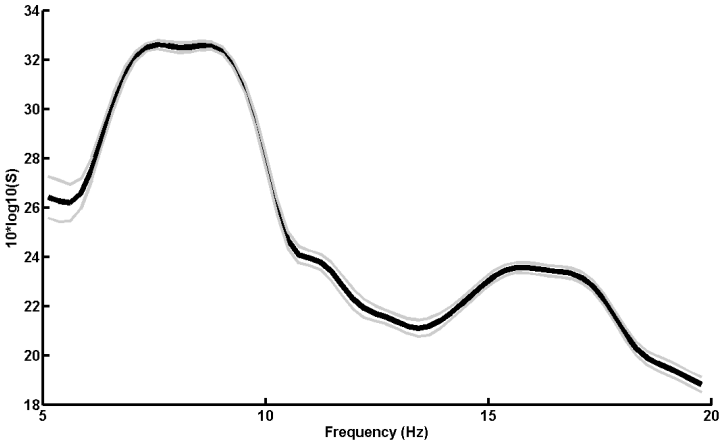

Figure 1: a) Hippocampal LFP Power Spectrum during Tactile discrimination task. b) Trial-average Power Spectrum of Hippocampal LFP of the last 600 msec before decision making.

a)

b)

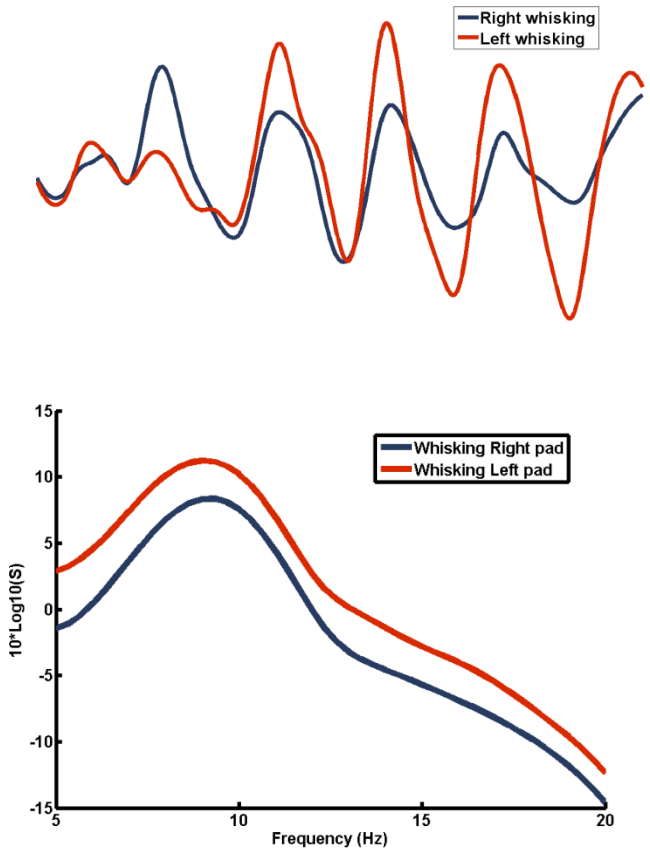

Figure 2: a) Whisking epoch during Tactile discrimination Task. b) Trial-average Power Spectrum of Whisking (right and left pad) during Tactile Discrimination Task.

Hippocampal LFP from the tactile guided task was compared with two control conditions: two out of three rats (rat 4 and 5) trained in the two texture tactile discrimination task were left to freely move around a rectangular platform for an average of 30 min each session (rat4: 5 session, rat5: 8 sessions) and the LFP power spectrum from two overt behaviors ('Walk' and 'Foot Planted') was computed separately. In this way we obtained a measure of theta power under motor action and motor quietness. In both cases LFP signal was cut into an average of 600msec epochs (termed 'trials'). Figure 3 shows the three conditions power spectrum. As expected, during motor action hippocampal theta power increased with respect to motor quietness. Interestingly, Walk period power spectrum was significantly higher than active discrimination epoch (Fig 4), suggesting that other factors more related to the cognitive processes at work apart from the motor movement may be governing theta activity during the task.

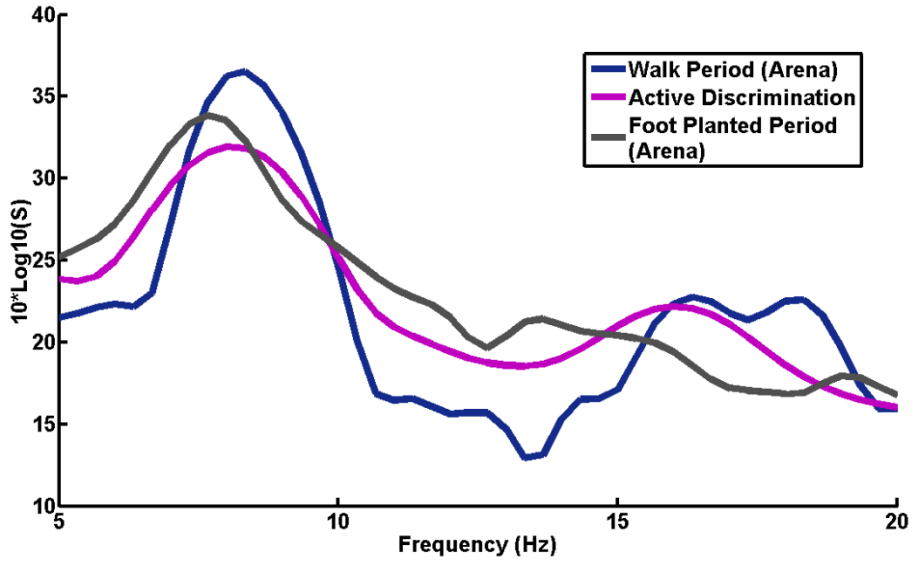

Figure 3: Trial-average Power Spectrum of Hippocampal LFP during Tactile Discrimination Task, Walk and Foot Planted epochs in the free moving arena.

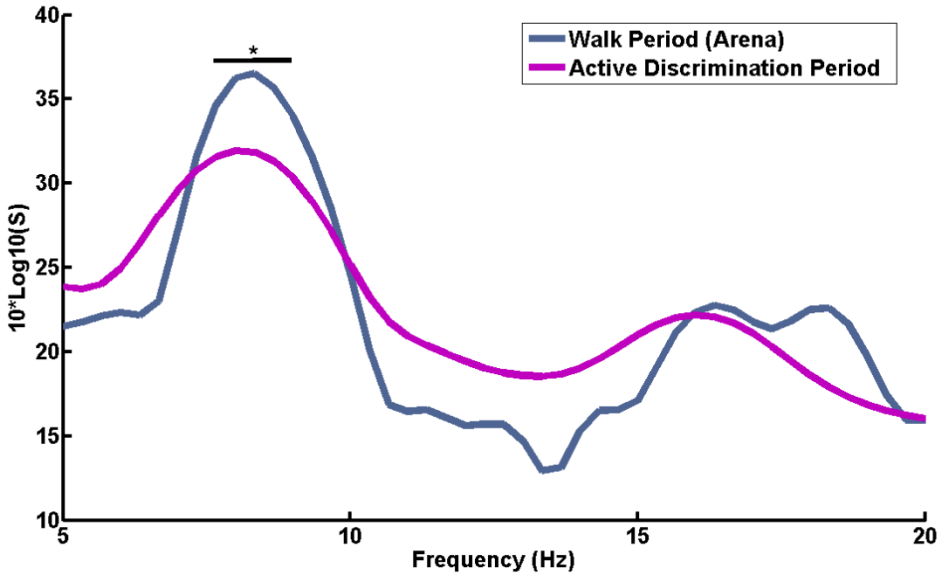

Figure 4: Trial-average Power Spectrum of Hippocampal LFP comparison of Tactile Discrimination Task vs Walk epochs in the Free moving Arena. Significant difference was computed by means of Montecarlo method ($p<0.05$, Bonferroni corrected, See Methods for details)

Whisking-Theta phase synchrony in the Texture Discrimination Task

As a means to study phase relationship between rhythmic movement of rat's vibrissae and hippocampal LFP during active discrimination task, we computed the trial-average PLV. As seen in figure 5 both rhythms were significantly locked for the frequency range 10-13Hz, whereas none of

the main frequencies, 8-9Hz for hippocampal theta and 9-10Hz for whisking, were significantly synchronized. We also studied the phase synchrony of exploratory whisking and hippocampal LFP when the rat was not performing a cognitive task but was actively moving in a platform. If the coupling of both signals were related to certain cognitive demands associated with reward, then synchronization at whatever frequency band should disappear as soon as the animal is not performing 'goal directed whisker movements'. As expected neither during Walk nor Foot planted epochs PLV was significant (Fig 6) at any of the frequency range evaluated.

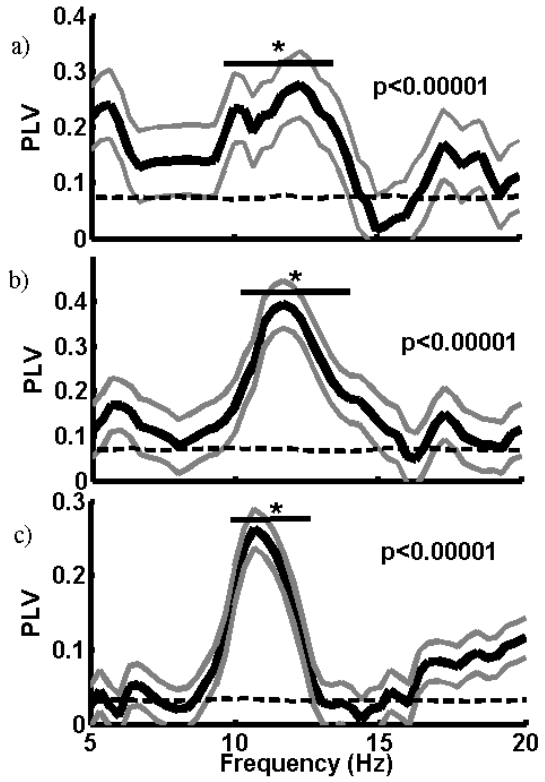

Figure 5: PLV during Tactile Discrimination Task. a) rat 3, b)rat 4, c) rat5. Statistical significance was computed by means of Montecarlo method. Dash line corresponds to the median value of the population drawn from 1000 shuffles across trial pairs. (All p<0.0001, Bonferroni corrected, rat3: n=128 rat4: n=148, rat5: n=686).

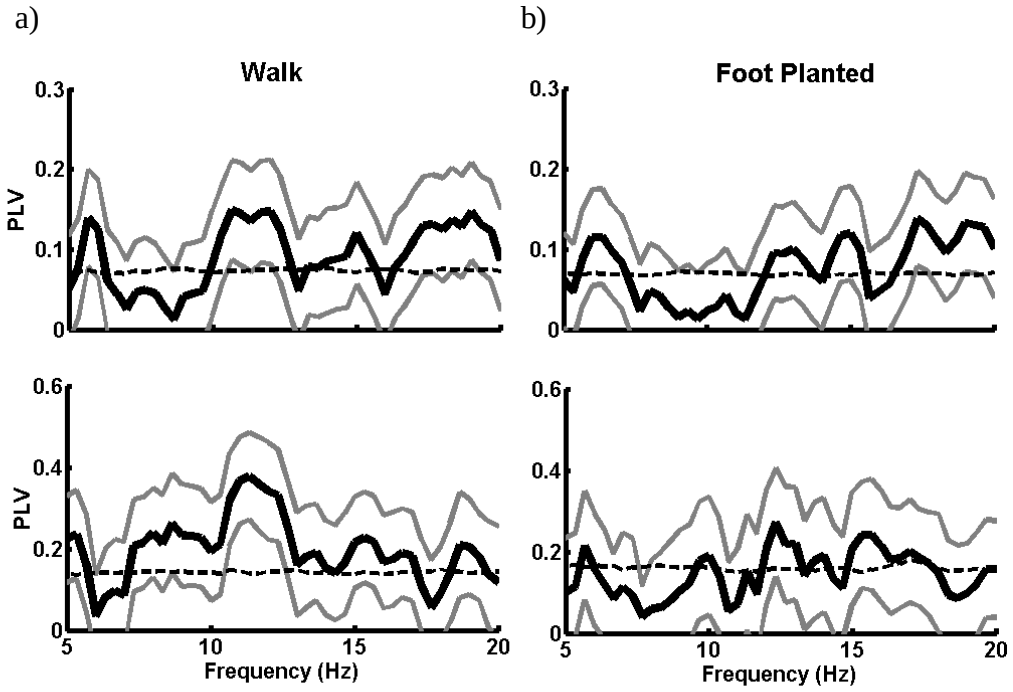

Figure 6: PLV during 'Walk' and 'Foot planted' epochs in the Free moving Arena. a) rat 4, b) rat 5. Statistical significance was computed by means of Montecarlo method. Dash line corresponds to the median value of the population drawn from 1000 shuffles across trial pairs. None of the conditions/animals were significant (p>0.001, Bonferroni corrected. rat4: n=127walk/n=144 foot planted, rat5: n=35walk/n=27foot planted).

Amplitude correlation between hippocampal Theta and Whisking

Independent of phase locking, it is possible that whisking and hippocampal theta rhythm activity can modulate each other on the time scale of individual epochs and this could be reflected in amplitude correlation. To test for this possibility, we performed a linear regression analysis between the peak spectral power in the contact whisking band (9.5Hz) with that in the theta rhythm (8.5 Hz) band to determine whether the two signals were statistically correlated (Fig. 7). Two out of three animals demonstrated a statistically significant correlation at the $p<0.05$ level. Although non conclusive, these results would indicate that the amplitudes of the two rhythmic signals are dependent of each other. Increasing the n would give us a better estimation of the amplitude coupling.

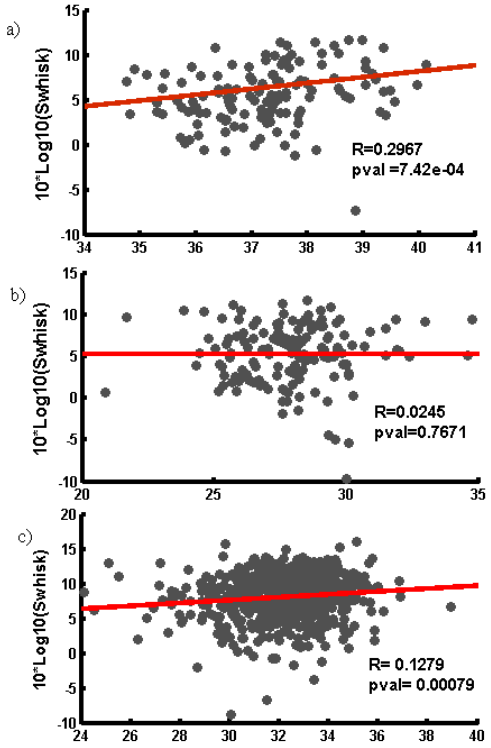

Figure 7: Amplitude Correlation between whisking and theta rhythm. Peak power of whisking versus peak power of hippocampal signal for: a) rat 3, b) rat 4, c) rat5. Each dot represents an average of 600msec trial. Correlation coefficient (Spearman) and pval associated for each animal indicated in the graph (Spearman correlation, $p<0.05$, rat3: n=128 rat4: n=148, rat5: n=686).

CONCLUSIONS AND DISCUSSION

In line with our study of phase relationship between primary somatosensory cortex and hippocampal theta we asked then whether whisking is synchronized to hippocampal theta rhythm when the animal is performing the tactile discrimination task. The somatosensory system of rats stands out by the fact that information collection is cyclical as rats protract and retract their whiskers ("whisking") in a rhythmic 10-Hz pattern. The notion that the coordination between brain areas might be related to the rhythmic of sensorimotor cycles is particularly appealing. Kleinfeld and colleagues studied whisker and LFP synchronization of different regions and found that 1) coherence between primary somatosensory cortex (LFP) and vibrissa motion triples when rats are engaged in a reward-based tasks (Ganguly K and Kleinfeld D , 2004), 2) whisking and CA1 theta rhythm are not coherent when the animal is exploring objects not associated to reward. Together these results suggest that phase relationship between whisking motion and oscillatory rhythms of the hippocampus may depend on the state of the animals as demonstrated in their first work. Here we provide evidence, that there is a certain degree of phase and amplitude relationship between whisking and hippocampal theta, and that this relationship disappears when the animal is not engaged in a goal-directed tactile task, but still actively whisking. Two striking points lie on the results: the first one is that phase synchrony is not observed all across the theta (5-12Hz) range but only confined to the 10-14Hz range. The second one, it is the lack of complete consistency across animals for the amplitude correlation. This last point could be easily disentangled by increasing the *n*. In doing so, we would statistically test whether the negative result can be considered an outlying measure. With respect to the first point, pretty much careful attention has to be applied. We will try in this discussion to shed some light on it: It could be thought that artifacts related to the spectral method filtered into the analysis. But how do we explain the fact that this synchronization disappears in the control conditions were data was treated in the same way. One possible explanation could be that data during active sensing is not really stationary, i.e. the joint probability distribution does not change when shifted in time. Even if the time length of the data analyzed is rather short (only four cycles of theta/whisking were analyzed in average) many factors like external stimulus and/or those related to the cognitive processes at work could be influencing the dynamic of theta oscillations. As we pointed out in the introductory chapter, many theta current dipoles are taking part in what is rather a complex but flexible global theta system (Sean M. Montgomery, Martha I. Betancur, and Gyorgy Buzsaki, 2009). Indeed, the dynamic spectrum shows some degree of change in the power of certain frequencies in the last 500msec before animal

withdrawal or decision making. Test for nonstationarity could help to disentangle these confounding results. If we rule out the non-stationary, then results simply show that only certain frequencies from the theta rhythm are actively coupled to whisking. As Buzsaki G pointed out in many publications (Buzaski G, 2006), taxonomy of brain oscillation should represent physiological entities generated by distinct entities, but unfortunately the exact mechanism of most of the brain oscillation are not known. Our observation could be an evidence for the complexity of oscillatory band classes, maybe generated by same molecular mechanisms but decoupled under certain circumstances. The neurobiological phenomenon underlying this process goes beyond the available experimental tools of this study. Still, they set precedence in this research direction.

Chapter V

General Discussion

GENERAL DISCUSSION

By testing phase-locking of somatosensory neurons to hippocampal theta together with whisking-hippocampal rhythm synchronization during a cognitive task and comparing them with control conditions, we were able to show, for the first time to our knowledge, that neurons from S1 and whisking couple to theta rhythm depending on the behavioral state of the animal. Somatosensory neurons and whisking activity are entrained to hippocampal theta rhythm when the animal is collecting meaningful tactile information from the environment.

A potential mechanism for such distant neurons may entail entorhinal cortex (EC) and/or PFC by way of their widespread and mostly reciprocal connections with primary (and secondary) sensory areas (Groenewegen HJ and Uylings HB, 2000), (Swanson LW and Kohler C, 1986), (Witter MP, 1993). Also sparse long-range hippocampal projections to distant neocortical regions could be responsible for imposing the hippocampal rhythmic output (Cenquizca LA and Swanson LW, 2007), (Jinno S, Klausberger T, Marton LF, Dalezios Y, Roberts JD, Fuentealba P, Bushong EA, Henze D, Buzsaki G and Somogyi P, 2007). But how hippocampus exerts its modulatory effect on whisking activity? Whisking-hippocampal rhythm coupling may be a consequence of coupling of any of the regions integrating the sensorimotor loops. Moreover, areas devoted to motivational processes as basal ganglia could be gating the entrainment during task related epochs. Although the thalamostriatal and corticostriatal pathways are well documented, their functions are less well studied. These connections are likely to operate in arousal and directing attention to behaviourally significant events (Smith Y, Raju DV, Pare JF and Sidibe M, 2004). Interestingly, although the basal ganglia (BG) are part of the sensorimotor loop (see (Kleinfeld D, Berg RW and O'Connor SM, 1999)) (Diamond ME, von Heimendahl M, Magne Knutsen P, Kleinfeld D and Ahissar E, 2008) forming a loop with superior colliculus and a higher order one with thalamus and S1, the role of BG in whisking is presently unclear. In the first loop, the superior colliculus sends projections to BG (subthalamic nucleus) (Hironobu Tokuno, Masahiko Takada, Yoshiaki Ikai and Noboru Mizuno, 1994) while it receives inhibitory projections from BG (substantia nigra, SN) (Niemi-Junkola UJ and Westby GW, 1998). S1 as well as S2, PV, parietal rhinal (PR) areas, posteromedial (PM) region and thalamus nuclei send projections to BG (dorsolateral neostriatum) (Alloway KD, Lou L, Nwabueze-Ogbo F and Chakrabarti S, 2006). Instead, BG sends descending projections to the ventrolateral domain of the VPM (VPMvl) which constitutes the extralemniscal pathway. In light of this evidence, BG could drive the sensorimotor system to goal directed whisking, which in consequence would be entrained rhythmically into the associative and memory systems.

Our results not only show that theta rhythms modulate the occurrence of S1 neuronal activity tuning its spiking activity in a specific time window, but also that neurons whose firing rate increased during contact with the stimulus had an opposite range of preferred phases compared to neurons whose firing rate did not increase above baseline levels. This implies that theta rhythm has an active participation on texture information by clustering neurons with increased firing rate. Which structure could take advantage of such entrainment? According to Buzsaki G (Buzsaki G, 2006, page 341), oscillatory entrainments of such long range multisynaptic regions are advantageous mainly for the hippocampus. By temporally biasing firing rate patterns of distanct cortical sites, well-timed messages from the same cortical areas will be treated preferentially over others. But in light of our last results, also primary and upstream processing sensory areas could take advantage of this entrainment; if the firing rate is the fundamental mechanism of texture conding information (Diamond ME, von Heimendahl M, Magne Knutsen P, Kleinfeld D and Ahissar E, 2008) then, clustering 'informative' spiking neurons to a certain time window and separating them from 'non-informative' neurons would increase the efficiency not only of information tranfer but also of information encoding/decoding. Further studies on this issue would be highlighting in the context of how the brain constructs a representation of meaningful stimuli.

Bibliography

Alloway KD, Lou L, Nwabueze-Ogbo F and Chakrabarti S. (2006). Topography of cortical projections to the dorsolateral neostriatum in rats: multiple overlapping sensorimotor pathways. *J Comp Neurol*, 499(1):33-48.

Arabzadeh E, Zorzin E and Diamond ME. (2005). Neuronal encoding of texture in the whisker sensory pathway. *PLoS Biol*, 3(1): e17.

Artola A and Singer W. (1993). Long-term depression of excitatory synaptic transmission and its relationship to long-term potentiation. *Trends Neurosci*, 16(11):480-7.

Batschelet E. (1981). *Circular Statistics in Biology.* London-NewYork: Academic Press Inc.

Benchenane K, Peyrache A, Khamassi M, Tierney PL, Gioanni Y, Battaglia FP and Wiener SI. (2010). Coherent theta oscillations and reorganization of spike timing in the hippocampal-prefrontal network upon learning. *Neuron*, 66:,921-936.

Berens P. (2009). CirStat: A MATLAB toolbox for Circular Statistic. *J of Statistical Software*, 31(10).

Berg RW, Whitmer D and Kleinfeld D. (2006). Exploratory whisking by rat is not phase locked to the hippocampal theta rhythm. *J Neurosci*, Jun 14;26(24):6518-22.

Bliss TVP and Collingridge GL. (1993). A synaptic model of memory: Long-Term potentiation in the hippocampus. *Nature*, 361, 31-39.

Bragin A, Jando G, Nadasdy Z, Hetke J, Wise K and Buzsaki G . (1995). Gamma (40-100 Hz) oscillation in the hippocampus of the behaving rat . *Journal of Neuroscience*, 15, 47-60.

Burwell RD and Amaral DG. (1998). Cortical afferents of the perirhinal, postrhinal, and entorhinal cortices of the rat. *J Comp Neurol*, 24;398(2):179-205.

Buzaski G. (2006). *Rhythms of the Brain.* Oxford, New York: Oxford University Press.

Cenquizca LA and Swanson LW. (2007). Spatial organization of direct hippocampal field CA1 axonal projections to the rest of the cerebral cortex. *Brain Res. Rev.* , 56, 1–26.

Csicsvari J, Jamieson B, Wise KD, Buzsaki G. (2003). Mechanisms of gamma oscillations in the hippocampus of the behaving rat. *Neuron*, 37(2):311-22.

Diamond ME, von Heimendahl M, Magne Knutsen P, Kleinfeld D and Ahissar E. (2008). 'Where' and 'what' in the whisker sensorimotor system. *Nature Revs Neurosc*, 9:601-612.

Dorfl J. (1982). The musculature of the mystacial vibrissae of the white mouse. *J Anat* , 135: 147-154.

Dorfl J. (1985). The innervation of the mystacial region of the white mouse. A topographical study. *J Anat*, 142: 173 184.

Eichenbaum H. (2000b). Hippocampus: Mapping or memory? *Current Biology* , 10, R785–R787.

Eichenbaum H, Dudchenko P, Wood E, Shapiro M and Tanila, H. (1999). The Hippocampus, Memory, Review and Place Cells: Is It Spatial Memory or a Memory Space? *Neuron*, 23, 209–226.

Engel AK, Fries P and Singer W. (2001). Dynamics Predictions: oscillations and synchrony in top-down processing. *Nature Reviews*, 2:708-21.

Ferbinteanu J and Shapiro ML. (2003). Prospective and retrospective memory coding in the hippocampus. *Neuron*, 40(6):1227-39.

Frank LM, Brown EN and Wilson M. (2000). Trajectory encoding in the hippocampus and entorhinal cortex. *Neuron*, 27(1):169-78.

Fries P, Womelsdorf T, Oostenveld R and Desimone R. (2008). The effects of visual stimulation and selective visual attention on rhythmic neuronal synchronization in macaque area V4. *J Neurosci*, 28(18):4823-35.

Fries, P. (2005). A mechanism for cognitive dynamics. Neuronal communication through neuronal coherence. *Trends Cogn Sci*, 9, 474–480.

Ganguly K and Kleinfeld D . (2004). Goal-directed whisking behavior increases phase-locking between vibrissa movement and electrical activity in primary sensory cortex in rat. *Proc Natl Acad Sci USA*, 101:12348 –12353.

Gray CM & McCormick DA. (1996). Chattering Cells: Superficial Pyramidal Neurons Contributing to the Generation of Synchronous Oscillations in the Visual Cortex. *Science*, 274 (5284): 109–13.

Groenewegen HJ and Uylings HB. (2000). The prefrontal cortex and the integration of sensory, limbic and autonomic information. *Prog. Brain Res.*, 126, 3–28.

Hironobu Tokuno, Masahiko Takada, Yoshiaki Ikai and Noboru Mizuno. (1994). Direct projections from the deep layers of the superior colliculus to the subthalamic nucleus in the rat. *Brain Research*, 639,1, 156-160 .

Hyman JM, Zilli EA, Paley AM, and Hasselmo ME. (2005). Medial prefrontal cortex cells show dynamic modulation with the hippocampal theta rhythm dependent on behavior. *Hippocampus*, 15:739–49.

Isomura Y, Sirota A, Ozen S, Montgomery S, Mizuseki K, Henze DA, and Buzsaki G. (2006). Integration and segregation of activity in entorhinal hippocampal subregions by neocortical slow oscillations. *Neuron* , 52, 871–882.

Itskov PM, Vinnik E and Diamond ME. (2011). Hippocampal Representation of Touch-Guided Behavior in Rats: Persistent and Independent Traces of Stimulus and Reward Location. *PLoS ONE*, 6(1): e16462.

Jarvis M and Mitra P. (2001). Sampling properties of the spectrum and coherency of sequences of action potentials. *Neural Computation*, 13(4), 717–749.

Ji D and Wilson MA. (2008). Firing rate dynamics in the hippocampus induced by trajectory learning. *J Neurosci*, 28(18):4679-89.

Jinno S, Klausberger T, Marton LF, Dalezios Y, Roberts JD, Fuentealba P, Bushong EA, Henze D, Buzsaki G and Somogyi P. (2007). Neuronal diversity in gabaergic long-range projections from the hippocampus. *J. Neurosci.*, 27, 8790–8804.

Johnson A and Redish AD. (2007). Neural ensembles in CA3 transiently encode paths forward of the animal at a decision point. *J Neurosci*, 27(45):12176-89.

Jones M and Wilson M. (2005). Theta Rhythms Coordinate Hippocampal-Prefrontal interactions in a spatial memory task. *Plos Biol*, 3(12): e402.

Kamondi A, Acsády L, Wang XJ and Buzsáki G. (1998). Theta oscillations in somata and dendrites of hippocampal pyramidal cells in vivo: activity-dependent phase-precession of action potentials. *Hippocampus*, 8(3):244-61.

Kerr KM, Agster KL, Furtak S and Burwell RD. (Hippocampus). *Functional Neuroanatomy of the Parahippocampal Region:The Lateral and Medial Entorhinal Areas.* 2007: 17:697–708.

Kleinfeld D, Ahissar E and Diamond ME. (2006). Active sensation: insights from the rodent vibrissa sensorimotor system. *Curr Opin Neurobiol*, 16(4):435-44.

Kleinfeld D, Berg RW and O'Connor SM. (1999). Anatomical loops and their electrical dynamics in relation to whisking by rat. *Somatosens Mot Res*, 16(2):69-88.

Lee AK and Wilson MA. (2006). Memory of sequential experience in the hippocampus during slow wave sleep. *Neuron*, 36(6):1183-94.

Lee MG, Chrobak JJ, Sik A, Wiley RG, Buzsaki G . (1994). Hippocampal theta activity following selective lesion of the septal cholinergic system. Neuroscience. *Neuroscience*, 62:1033-1047.

Lepage KQ, Kramer MA, Eden UT. (2011). The dependence of spike field coherence on expected intensity. *Neural Computation*, 23, 2209–2241.

Leutgeb S, Leutgeb JK, Barnes CA, Moser EI and McNaughton BL. (2005). Independent codes for spatial and episodic memory in hippocampal neuronal ensemb;es. *Science*, 309: 619–623.

Louie K and Wilson MA. (2001). Temporally structured replay of awake hippocampal ensemble activity during rapid eye movement sleep. *Neuron*, 29(1):145-56.

Macrides F, Eichenbaum HB, Forbes WB. (1982). Temporal relationship between sniffing and the limbic theta rhythm during odor discrimination reversal learning. *J Neurosci*, 12:1705–1717.

Mardia KV and Jupp PE. (2000). *Directional Statistics.* Chichester: John Wiley & Sons, Ltd.

Markram H, Lübke J, Frotscher M and Sakmann B. (1997). Regulation of synaptic efficacy by coincidence of postsynaptic APs and EPSPs. *Science*, 275(5297):213-5.

Marr D. (1971). Simple memory: a theory for archicortex. *Philosophical Transactions of the Royal Society of London.Series B, Biological Sciences*, 262, 23-81.

Mitzdorf U. (1985). Current source–density method and application in cat cerebral cortex: investigation of evoked potentials and EEG phenomena. *Physiol Rev*, 65:37–100.

Miyashita E, Keller A and Asanuma H. (1994). Input- output organization of the rat vibrissal motor cortex. *Exp Brain Res*, 99: 223-232.

Moita MA, Rosis S, Zhou Y, LeDoux JE and Blair HT. (2004). Putting fear in its place: remapping of hippocampal place cells during fear conditioning. *J Neurosci*, 24(31):7015-23.

Montgomery SM, Betancur MI and Buzsaki G. (2009). Behavior-Dependent Coordination of Multiple Theta Dipoles in the Hippocampus. *The Journal of Neuroscience*, 29(5):1381–1394.

Naber PA, Witter MP and Lopes Silva FH. (2001). Evidence for a direct projection from the postrhinal cortex to the subiculum in the rat. *Hippocampus*, 11(2):105-17.

Nadel L, Samsonovich A, Ryan L and Moscovitch M. (2000). Multiple trace theory of human memory: computational, neuroimaging, and neuropsychological results. *Hippocampus*, 10, 352–368.

Nadel L and Moscovitch M. (1997). Memory consolidation, retrograde amnesia and the and the hippocampal complex. *Current Opinion in Neurobiology*, 7,217-227.

Niemi-Junkola UJ and Westby GW. (1998). Spatial variation in the effects of inactivation of substantia nigra on neuronal activity in rat superior colliculus. *Neurosc Lett*, 241: 175-179.

O'Keefe J, Nadel L. (1978). *The hippocampus as a cognitive map*. Oxford; New York: Clarendon Press; Oxford University Press.

O'Keefe J and Dostrovsky J. (1971). The hippocampus as a spatial map: Preliminary evidence from unit activity in the freely-moving rat. *Brain Research, Vol 34, 1971, 171-175*, 34, 171-175.

Pedemonte M, Velluti RA. (2005). El procesamiento sensorial podría estar organizado en el tiempo por ritmos cerebrales ultradianos. *Rev Neurol*, 40 (3): 166-72.

Penttonen M, Buzsaki G. (2003). *Thalamus and Related Systems*, 2, 145.

Pereira A, Ribeiro S, Wiest M, Moore LC, Pantoja J, Lin S and Nicolelis MA. (2007). Processing of tactile information by the hippocampus. *PNAS*, 18286-291.

Perkon I, Kosir A, Itskov PM, Tasic J and Diamond ME. (2011). Unsupervised quantification of whisking and head movement in freely moving rodents. *J Neurophysiol*, 105(4):1950-62.

Petersen CCH. (2007). The Functional Organization of the Barrel Cortex. *Neuron* , 56, 339-355.

Sean M. Montgomery, Martha I. Betancur, and Gyorgy Buzsaki. (2009). Behavior-Dependent Coordination of Multiple Theta Dipoles in the Hippocampus. *The Journal of Neuroscience* , 29(5):1381–1394 .

Sesack SR and Grace AA. (2010). Cortico-Basal Ganglia reward network: microcircuitry. *Neuropsychopharmacology*, 35(1):27-47.

Siapas AG, Lubenov EV and Wilson MA. (2005). Prefrontal Phase Locking to Hippocampal Theta Oscillations. *Neuron*, 46, 141–151.

Sirota A, and Buzsaki G. (2007). . (2007). Interaction between neocortical and hippocampal networks via slow oscillations. . *Thalamus Relat. Syst.* , 3, 245–259.

Sirota A, Montgomery S, Fujisawa S, Isomura Y, Zugaro M and Buzsáki G. (2008). Entrainment of neocortical neurons and gamma oscillations by the hippocampal theta rhythm. *Neuron*, 60(4):683-97.

Smith Y, Raju DV, Pare JF and Sidibe M . (2004). The thalamostriatal system: a highly specific network of the basal ganglia circuitry. *Trends Neurosci*, 27:520-527.

Squire L and Zola-Morgan S. (1991). The medial temporal lobe memory system. *Science* , 253,1380-1386.

Stella F, Cerasti E, Si B, Jezek K and Treves A. (2011). Self-organization of multiple spatial and context memories in the hippocampus. *Neuroscience & Biobehavioral Reviews*, Submitted.

Swanson LW and Kohler C. (1986). Anatomical evidence for direct projections from the entorhinal area to the entire cortical mantle in the rat. *J. Neurosci.*, 6, 3010–3023.

Ulrich D. (2002). Dendritic resonance in rat neocortical pyramidal cells . *J. Neurophysiol.* , 87, 2753–2759.

von Heimendahl M, Itskov PM, Arabzadeh E and Diamond ME. (2007). Neuronal activity in rat barrel cortex underlying texture discrimination. *PLoS Biol*, 5(11): e305.

Wallenstein GV, Eichenbaum H and Hasselmo ME. (1998). The hippocampus as an associator of discontiguous events. *Trends Neurosci*, 21, 317–323.

Wise RA. (2004). Dopamine, learning and motivation. *Nat Rev Neurosci* , 5: 483–494.

Witter MP. (1993). Organization of the entorhinal-hippocampal system: a review of current anatomical data. *Hippocampus*, 3:33-44.

Witter MP and Amaral DG. (1991). Entorhinal cortex of the monkey: V. Projections to the dentate gyrus, hippocampus, and subicular complex. *J Comp Neurol*, 15;307(3):437-59.

Witter MP and Moser EI. (2006). Spatial representation and the architecture of the entorhinal cortex. *Trends Neurosci*, 29(12):671-8.

Witter MP, Wouterlood FG, Naber PA and Van Haeften T. (2000). Anatomical organization of the parahippocampal-hippocampal network. *Ann N Y Acad Sci*, 911:1-24.

Wood ER, Dudchenko PA, Robitsek RJ and Eichenbaum H. (2000). Hippocampal neurons encode information about different types of memory episodes occurring in the same location. *Neuron*, 27(3):623-33.

Woolsey TA and Van der Loos H. (1970). The structural organization of layer IV in the somatosensory region (SI) of mouse cerebral cortex. The description of a cortical field composed of discrete cytoarchitectonic units. *Brain Res*, 17(2):205-42.